Proposal for a predictive model for micropiles bond resistance based on load tests

Case study: Analysis in fine-granular soils of La Ceja, Antioquia – Colombia

MAURICIO ALEJANDRO MOLANO QUIROZ

TESIS

Asesor, docente
DANIEL FELIPE RUIZ RESTREPO

UNIVERSIDAD EAFIT
ESCUELA DE CIENCIAS APLICADAS E INGENIERÍA
MAESTRÍA EN INGENIERÍA
MEDELLÍN
2026

UNIVERSIDAD EAFIT

Proposal for a predictive model for micropiles bond resistance based on load tests

Case study: Analysis in fine-granular soils of La Ceja, Antioquia – Colombia

Mauricio Molano Quiroz

Abstract

The use of micropiles has gained increasing popularity in Latin America as a foundation system due to their versatility, ease of installation in complex conditions, and growing load-bearing capacity, driven by the availability of specialized equipment, materials, advanced technologies, technical expertise, and a maturing culture of load testing. This allows the designers to reduce uncertainty, particularly from the geotechnical perspective, specifically when comparing them with other foundation systems commonly used in the region.

Additionally, the increased implementation of both verification and quality control static load test programs commonly known as verification test and proof test based on the definition presented in the FHWA document for Design and Construction of Micropiles [1], has made it possible to collect sufficient data for estimating design parameters, developing predictive models, and implementing Reliability-Based design (RBD) approaches across different soil conditions. This approach enables optimized solutions that are better adapted to specific loading, geotechnical and geological conditions. This considers the possibility of proposing site resistance factors for geotechnical design of micropiles as mentioned in [2].

To develop the model proposal presented in this study, various tasks were carried out to characterize the geotechnical conditions of the site and to assess the load-deformation behavior of micropiles subjected to tension, compression, and lateral loads. This information served as the foundation for building a strategic framework that allows a comprehensive methodology for the development of a predictive model adaptable to different site conditions considering the information available and allowed comparisons between different construction techniques and their associated skin friction resistance represented in literature as α_{bond} or τ (tau).

A total of 40 load tests were collected and analyzed, located in the fine alluvial deposit zone of the La Pereira stream in the municipality of La Ceja, Antioquia. These tests were performed using two different installation techniques on two different sites in the same geotechnical and geological environment which permit stablish comparison between the two sites. The techniques used were self-drilling micropiles (simultaneous drilling and grouting), and pre-drilled micropiles with Type B or Type

C injection, based on the classification presented in [1]. This dual approach enabled comparative analysis of behavior and ground to grout adhesion for different cases regarding injection type and load application (compression and tension). With the purpose of validating and as a benchmark values, additional load test reaching failure were included from other sites.

Keywords: Micropiles, static load testing, compression, tension, empirical methods, load capacity, unit shaft resistance, predictive models.

Introduction

Current micropiles design methodologies are still mainly based on preliminary values from empirical correlations such as those proposed by FHWA [1], which relies on soil type and grouting method to estimate ground to grout bond resistance. This first approach based on the recommendations of [1] is inherently uncertain with general values and is usually used as an initial approximation for preliminar designs. Another commonly used method developed by Bustamante and Doix [3], which uses SPT blow counts (N-values) as input can lead to a more particular approximation considering site specific N-values for the estimations and including injection type as well as input data. Other methods that consider specific geotechnical information such as *alpha – method* are also commonly used with the disadvantage of requiring robust laboratory information specially for stratified soils. The “alpha method” is widely used in cohesive soils, linking undrained shear strength (Su) with a factor α_{bond} to estimate unit shaft resistance. Such predictive correlations involving Su are well-documented in recent studies [4].

Recent literature such as J.E. Loehr, A.Z. Boeckmann, and D. Ding [2] defines those as "presumptive" and “predictive” methods. The same document discusses alternative approaches, including methods based on site specific load tests that can lead to reduce uncertainties and therefore to higher resistance factors.

Load test-based methods also offer valuable information that can be gathered alongside with the basic load-test information, being a pathway for directly determining unit shaft resistance from actual performance. Recent Reliability-Based Design (RBD) frameworks adjust resistance factors based on how shaft resistance is estimated by assigning lower factors from 0.2 to 0.4 for presumptive methods, and higher values approaching 1.0 for predictive or load-test-based methods, especially when supported by substantial field data.

Another important factor is the micropiles construction method. Two general categories can be defined:

- Pre-drilled micropiles with type C or D grouting (also known as repetitive injection systems IR or IRS)
- Self-drilling micropiles with type B or E grouting (also known as IGU – Global One-Step Injection)

Recent research, such as studies by A.Y. Abd Elaziz and M.H. El Naggar [5], has focused on the performance of self-drilling micropiles considered in literature as type B or type E micropiles. It is worth mentioning that presumptive methods typically assign higher shaft resistance values to repetitive injection systems (IR/IRS).

Regarding the load transfer along micropiles shaft, studies such as M. N. Elsiragy, *"Comparative Investigation of Loading Test on Micro-Piles Installed with Different Technique – (Case Study),"* [6] and A. Misra, C.-H. Chen, R. Oberoi y A. Kleiber*, "Simplified Analysis Method for Micropiles Pullout Behavior* [6] have compared axial behavior between different installation techniques aiming to understand the unit skin friction resistance on micropiles. Retro-analysis of load tests (including those that do not reach failure) has also been used to estimate unit shaft resistance [7]. Understanding load transfer along the micropiles shaft is critical—especially in stratified soils. For this purpose, two primary methods are used: Instrumentation along the micropiles with strain gauges and numerical modeling [8].

Considering the aspects mentioned, the current design flow of micropiles may present advantages especially for preliminar calculations when using presumptive methods and existing predictive methods if enough geotechnical information is available. Although, that current methods allow the generation of initial alternatives to be tested, the decision-making process still requires more complex and detailed information such as instrumented micropiles with strain gauges, finite element analysis and finite differences analysis that also requires robust and reliable field and laboratory information. These conditions imply the necessity of additional geotechnical information and load – test data that is rarely available in the common practice, which presents opportunities for the proposal of alternative frameworks to predict, analyze and calibrate unit skin resistance and resistance factors for more comprehensive and realistic designs.

For these purposes, static load test data whether failure is achieved or not can be used to calibrate resistance factors. This calibration process and associated statistical methods are presented in [9], [10], and [11].

Finally, this study aims to quantify the relationship between field parameters such as N-SPT and Vs as an explanatory variables and unit bond resistance (τ) in fine-grained alluvial deposits, and to calibrate a reliability-based resistance factor (ϕ) suitable for LRFD design. Having the option to correlate skin friction resistance with N-spt and Vs gives an additional predictive alternative even when only shear wave velocity, Vs is available. Additionally, a comprehensive and adaptable framework is proposed to estimate the load transfer and skin friction resistance along micropiles shaft, allowing designers understand the resistance along micropiles in stratified soils for a more reliable decision – making.

Model Framework

To develop the model a specific workflow was defined as a decision-making tool, to understand based on the information available how to estimate the parameter and build the regression models to find correlation between the explanatory variables and the unit skin friction resistance or shaft resistance along the micropiles estimating the variation of the load transference. In figure 1, the workflow for the implementation of the model is presented.

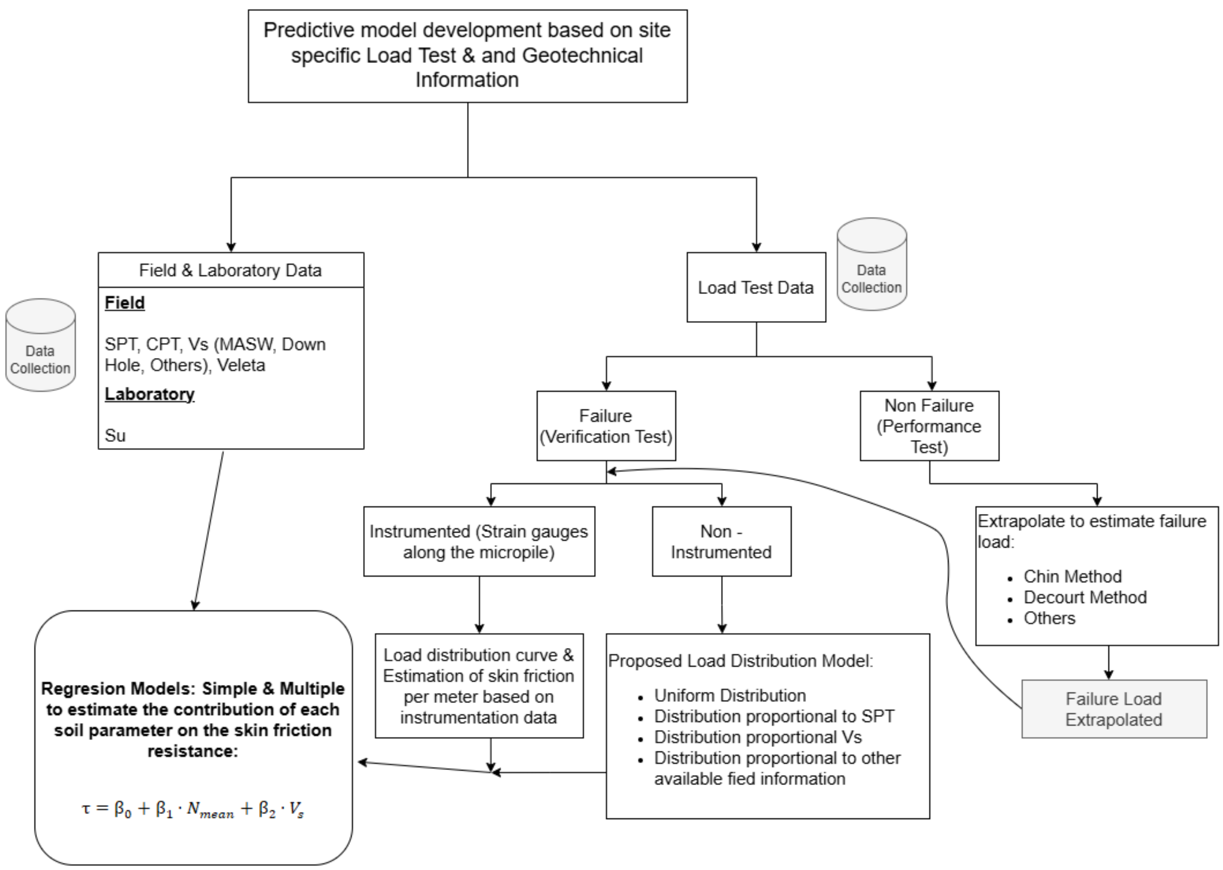

Figure 1. Model framework and workflow scheme

This workflow starts by understanding the availability of geotechnical information from the field and laboratory tests and the information collected from load tests whether the tests were in tension, compression, reaching failure or not. It is important to note that the availability of instrumented load tests with strain gauge or other devises that allow the estimation of load transfer directly is very uncommon hence alternatives such as numerical models or proportional assignation based on N-spt or Vs as proposed in this model are viable alternatives to improve the models when information is limited.

Two key steps for the development of the model are: 1. The estimation of unit skin friction along micropiles shaft when data from instrumentation is not available and 2. The extrapolation process to estimate the failure load in those cases where the tests did not reach failure.

1. To estimate the unit skin friction along micropile shaft based on data from N-spt and Vs from MASW, the following process was carried out.

- Initial estimation of τ or qs through back-analysis by using the test load (whether reaching failure or not)

  • Divide the micropile into segments of 1 meter.

  • Assign a value of N-spt and Vs to each segment based on field data.

- Calculate an average unit shaft resistance (τ or qs) based on the mobilized load and the lateral surface area of the micropile.

$$\tau_{avg} = \frac{Q_{ult}}{\pi \cdot d \cdot L}$$

Where:

- Qult: ultimate load measured in the test
- *d*: diameter of the micropile,
- *L*: total length.

Apply a load transfer model for average skin friction resistance (proportional to N-spt or Vs), to estimate the unit skin friction resistance along the length of the micropile on each segment.

Based on SPT:

$$\tau_i = \tau_{avg} \cdot n \cdot \frac{N_{spt,i}}{\sum N_{spt}}$$

Based on shear wave velocity:

$$\tau_i = \tau_{avg} \cdot n \cdot \frac{V_{s,i}}{\sum V_s}$$

Where:

- n: number of pile segments
- V_s: average shear wave velocity
- $N_{-spt:}$ average standard penetration tests blow count

This approach was applied using the average unit shaft resistance mobilized at the Test Load (TL) level for tension and compression load tests.

2. The extrapolation process to estimate the failure load in those cases where the tests did not reach failure.

The obtain the Test Load (TL) at failure, extrapolation process is central to complete the data collection especially when information from load test reaching failure is limited. For this purpose, several extrapolation methos can be evaluated to select the best alternative. For this selection, methods such as Chin – Kondner (1970) [12], Decourt (1995) [13], J. B. Hansen (1968) [14], Davisson (1972) [15] among others might be considered.

Additionally, load tests from other sites, even from different geotechnical conditions can be included to validate the extrapolation methods, due to the possibility to compare those additional load tests to failure with the predictions from the different extrapolation methods. Consequently, it is important to implement a progressive analysis by cutting the data at different points and running the extrapolation to check the feasibility of each method.

Finally, once the data set is completed, the regression models must be implemented Thus, an initial approximation is proposed through a multiple linear regression model, as follows:

$$\tau = \beta_0 + \beta_1 \cdot N_{mean} + \beta_2 \cdot V_s$$

Where:

- τ: unit skin friction resistance (in kPa),
- N_{mean}: average SPT blow count,
- V_s: shear wave velocity (in m/s),
- $\beta 0$: model intercept (baseline value),
- $\beta 1, \beta 2$: coefficients indicating how much τ changes per unit increase in N or V_s

Similarly, other simple regression models using N-SPT and V_s independently can also be developed, as well as more advanced machine learning models such as Random Forest. In any case, the quality and quantity of available data are critical to improving the predictive power of the models. Additionally, cross-validation should be performed to assess the models' predictive capabilities and to ensure the physical relevance of the input variables for both shear wave velocity (Vs) and standard penetration resistance (N-spt) that might have explanatory value in estimating unit skin friction resistance on micropiles.

In the case of the current model under development, the use of N-SPT and Vs values alone as input parameters to estimate a potential distribution of unit skin friction along the micropile, proportional to them, allows the building of preliminary predictions. These predictions can later be validated using additional load test data or available information from different sites with similar geotechnical environments.

Case study: Analysis in fine-granular soils of La Ceja, Antioquia – Colombia

The present case study consists of two sites in which micropile foundations were implemented, both sites in a similar geotechnical and geological environment. The sites studied are in the fine alluvial deposit zone of the La Pereira stream in the municipality of La Ceja, Antioquia. In figure 2, the location of the sites is shown.

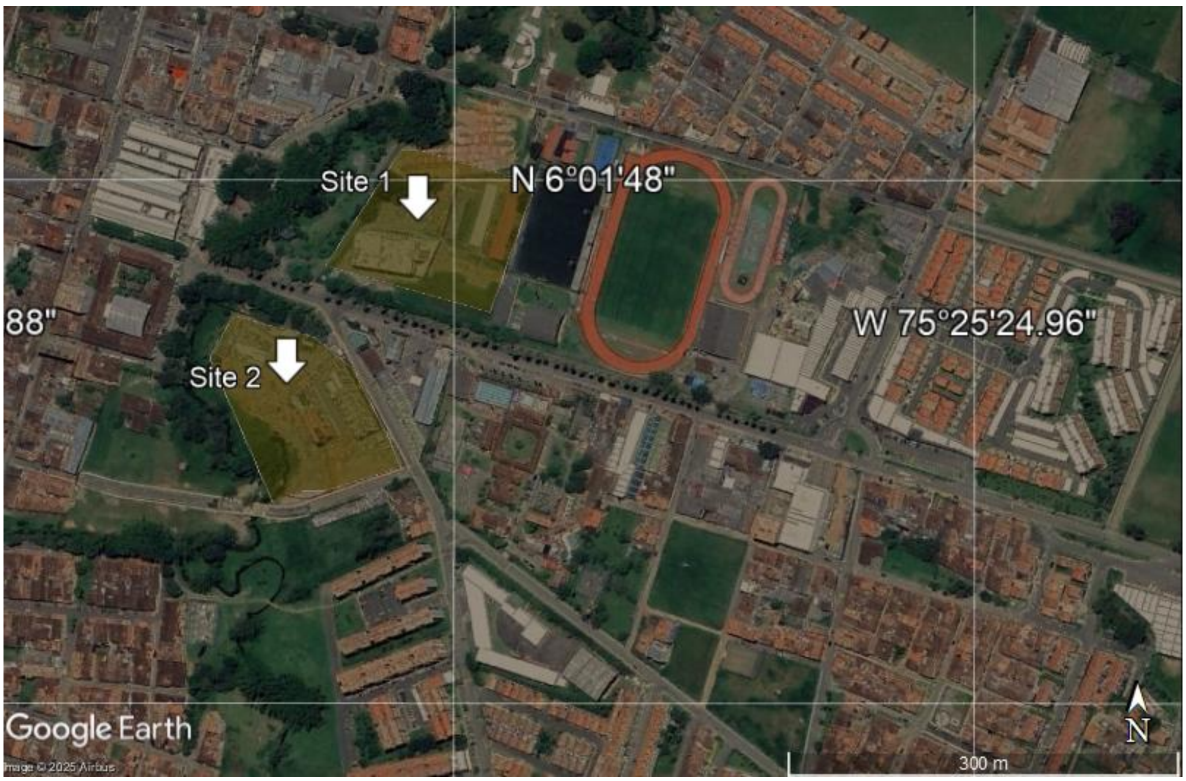

Figure 2. Location Site 1 & Site 2

Geotechnical Site Characterization

The geotechnical profile corresponds to a sequence of eolic (volcanic ash) and alluvial (fine-grained) deposits, associated with floodplains and peat layers, underlain by deeper alluvial strata. The average stratigraphy is shown in the figure 3. Then the description, average parameter and the variation of N-spt and Vs values with depth are presented in figure 4. The thickness of each layer identified are approximately 2 meters for the volcanic ash layer, 2 meters for the fine alluvial layer, and from 4 meters down to the explored depth (-15 m), a fine to medium alluvial deposit is observed.

D (m)	Soil Description
0,3 **0,5** **1,00** 1,45	Volcanic ash; brown, **clayey silt** with black mottling. Contains roots. High plasticity
2,00 2,45 **3,00** 3,45	Floodplain (alluvial) deposit: brown **silty clay** (USCS CH–CL) with black mottling. Mixed with organic matter. High plasticity.
4,45 5,45 6,45 7,45 8,45 9,45 10,45 11,45 12,45 13,45 14,45 15,50	Alluvial deposit with interbeds of **fine- to medium-grained sandy silt clay and gravel** (USCS SM–SC–GM); grayish-brown to grayish-green. Contains subrounded rock fragments from millimeter to centimeter scale. Low to non-plastic

Volcanic Ash
Unit weight: γ = 16.00 kN/m^3
Internal friction angle: φ_{ef} = 5.0°
Cohesion: c_{ef} = 20.0 kPa
Poisson's ratio: ν = 0.40
Deformation modulus: E_a = 2.00 MPa
Saturated unit weight: γ_{sat} = 18.00 kN/m^3
Soil type: = cohesive

Floodplain Deposit
Unit weight: γ = 18.00 kN/m^3
Internal friction angle: φ_{ef} = 30.0°
Cohesion: c_{ef} = 5.0 kPa
Poisson's ratio: ν = 0.34
Deformation modulus: E_a = 15.00 MPa
Saturated unit weight: γ_{sat} = 19.50 kN/m^3
Soil type: = cohesive

Medium Alluvial Soil
Unit weight: γ = 18.50 kN/m^3
Internal friction angle: φ_{ef} = 30.0°
Cohesion: c_{ef} = 5.0 kPa
Poisson's ratio: ν = 0.34
Deformation modulus: E_a = 15.00 MPa
Soil type: = cohesive

Figure 3. Geotechnical parameters & Stratigraphy

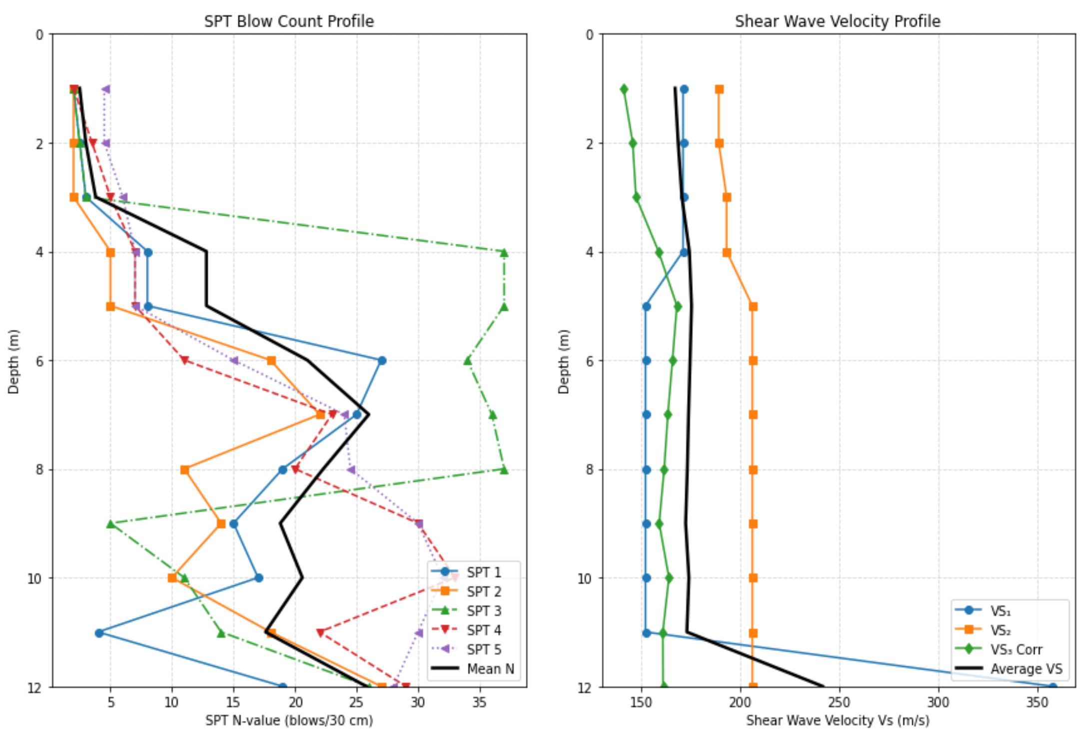

(a) (b)

Figure 4. (a) Variation of N-spt with depth and (b) Vs values with depth

Load test records

A total of 40 tests results were collected, primarily axial compression and tension tests. All 40 tests were carried out across two projects located in the same area of the municipality of La Ceja, under similar geotechnical conditions as determined by the site investigations conducted for each test. Only two of the 40 tests achieve failure which is a limitation for the analysis in this research. More tests achieving failure were collected as complementary information for validation purposes. In table 1, the summary of the results is presented. The complete information is presented as an appendix. Additionally, the curves load (kN) vs Settlement (mm) are presented in figure 5.

It is worth mentioning that the information presented in the table presented shows the summary and characterization of the load test records used in the present study, including to main point to build the load vs deformation curves as well as the diameter and length ranges of the micropiles. Additionally, it is important to note that the third load test to failure included is part of a different project located in a different municipality with a similar geotechnical environment. It was used to validate some of the assumptions used during this preliminary development. Different analysis can be done with the data related to the unloading process, especially the values of the elastic recovery of micropiles tested.

Table 1. Load Test and micropiles summary

Category	Sub.Category	Quantity	Max Settlement at DL [mm]	Max Settlement at TL [mm]	Diameter range (mm)	Lenght range (m)
Test Type	Compression Tests	13	5	24	150 - 200	10 to 12
Test Type	Tension Tests	27	9	15,7	150 - 200	10 to 12
Micropile Type	Hollow Bar	22	5	24	150 - 200	10 to 12
Micropile Type	Type D	18	9,5	15,7	150 - 200	10 to 12
Performance	Tests to Failure	3	9,5	24	150 - 200	10 to 12
Performance	Non-Failure Tests	37	9	15,7	150 - 200	10 to 12
Performance	Total Load Tests	40	9,5	24	150 - 200	10 to 12

In general, at Design Load (DL) and Test Load (TL), the settlements recorded were under 25,4mm for those at TL which is a threshold value and used as a reference in the common practice of foundation design. As mentioned, in figure 5, the deformation for tension test is presented as an uplift deformation, and for compression test is presented as settlement.

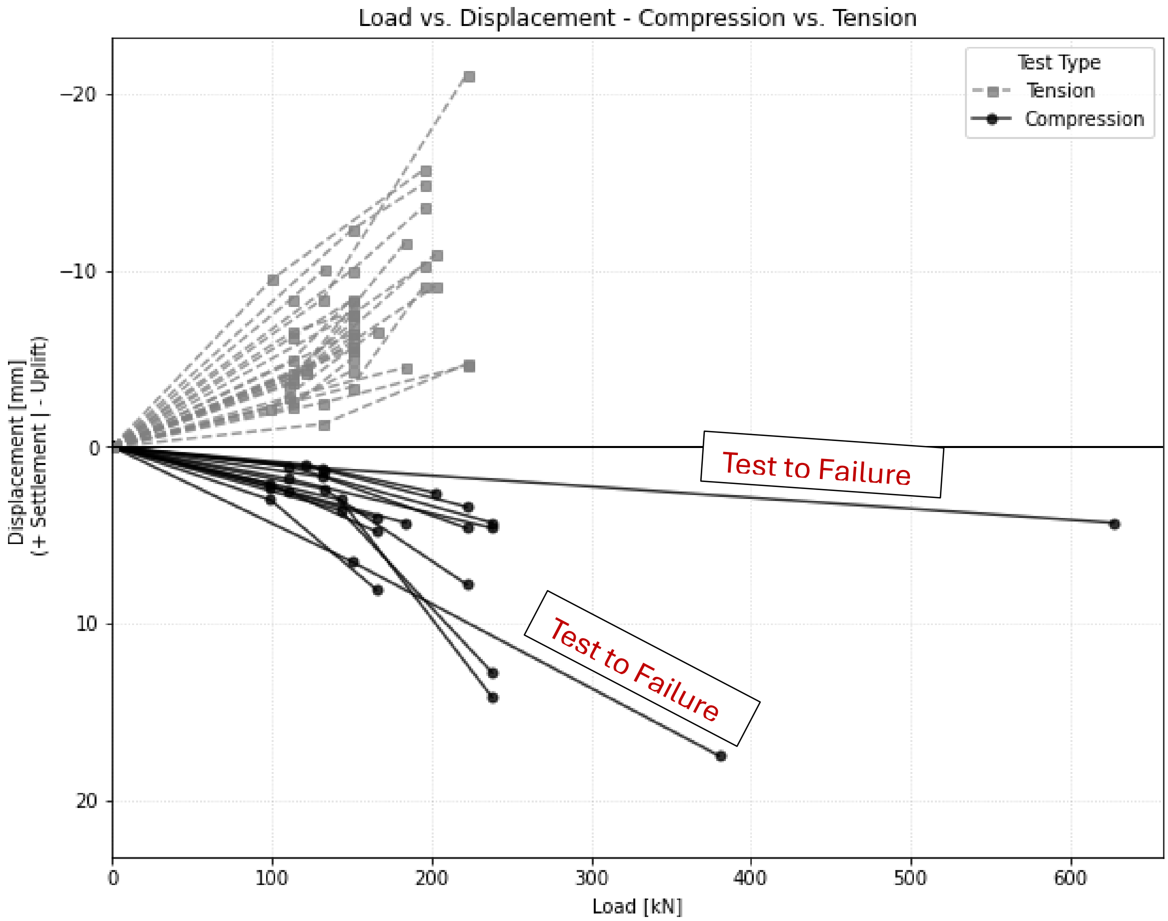

Figure 5. Load (kN) Vs Settlement/Uplift (mm)

Extrapolation methods

As mentioned before, additional load tests from different geotechnical conditions were considered to validate the extrapolation methods, due to the possibility to compare additional load tests to failure. For the selection of the method used for extrapolation, several methods were evaluated such as Chin – Kondner (1970) [12], Decourt (1995) [13], J. B. Hansen (1968) [14], Davisson (1972) [15] among others. From that evaluation Chin and Decourt were the best predictors after several trials using loads tests reaching failure and cutting the data at different points to check the prediction power of each method. In table 2 shown below, the cases analyzed are shown.

Table 2. Extrapolation Progressive Analysis. Chin (1970) & Decourt (1995)

Test		Load (kN)	Settlement (mm)	Q_ult (Chin) [kN]	%Error	Q_ult (Decourt) [kN]	%Error
Test 1	Validation 1	263,4	5,07	572	-8,9%	518	17,5%
	Validation 2	395,1	10,18	770	22,7%	716	-14,1%
	Real Failure	627,7	17,00				
Test 2	Validation 1	757,0	5,94	1582	-1,2%	1278	20,2%
	Validation 2	1019,0	8,54	1819	13,6%	1622	1,3%
	Validation 3	1164,0	10,96	2247	40,3%	1965	22,7%
	Real Failure	1601,0	23,13				

The progressive validation revealed a critical inflection point in the predictive models. At a deformation of approximately 10 mm, the reliability of the hyperbolic methods (Chin and Decourt) begins to degrade. Beyond this threshold, their predictions started to diverge significantly from the measured performance, consistently overestimating the ultimate capacity. This finding suggests a practical limit to their applicability; while these methods are robust for modeling behavior at moderate strains, their underlying hyperbolic assumption loses fidelity as the micropiles approaches an advanced failure state where more complex soil mechanics govern the response.

Considering this condition, before implementing the extrapolation methods, the settlement at tested load was verify to ensure that in every case the settlement were under 10mm to avoid overestimating the ultimate load and as a result, none of the extrapolated tests resulted in ultimate load higher that the loads reached in the tests conducted to failure available in both micropiles type analyzed: MP6 (Type D) and MP21 (Hollow Bar). This consideration resulted in a conservative measure, obtaining values likely to be underestimation of the actual micropiles shaft resistance. However, for the compression tests, that underestimation might be compensated with the negligible tip resistance assumed in the common practice.

In figure 6, the load tests records are presented after Chin Method implemented for those tests that did not reach failure. For the extrapolation, the reference value of 25,4mm (1”) was considered as a threshold point from which the micropile starts a plastic zone, so is defined as a potential failure point. As mentioned before, alternative methods such Chin – Kondner (1970) [12], Decourt (1995) [13], J. B. Hansen (1968) [14], Davisson (1972) [15] were evaluated, eventhough, only Chin in shown in the figure.

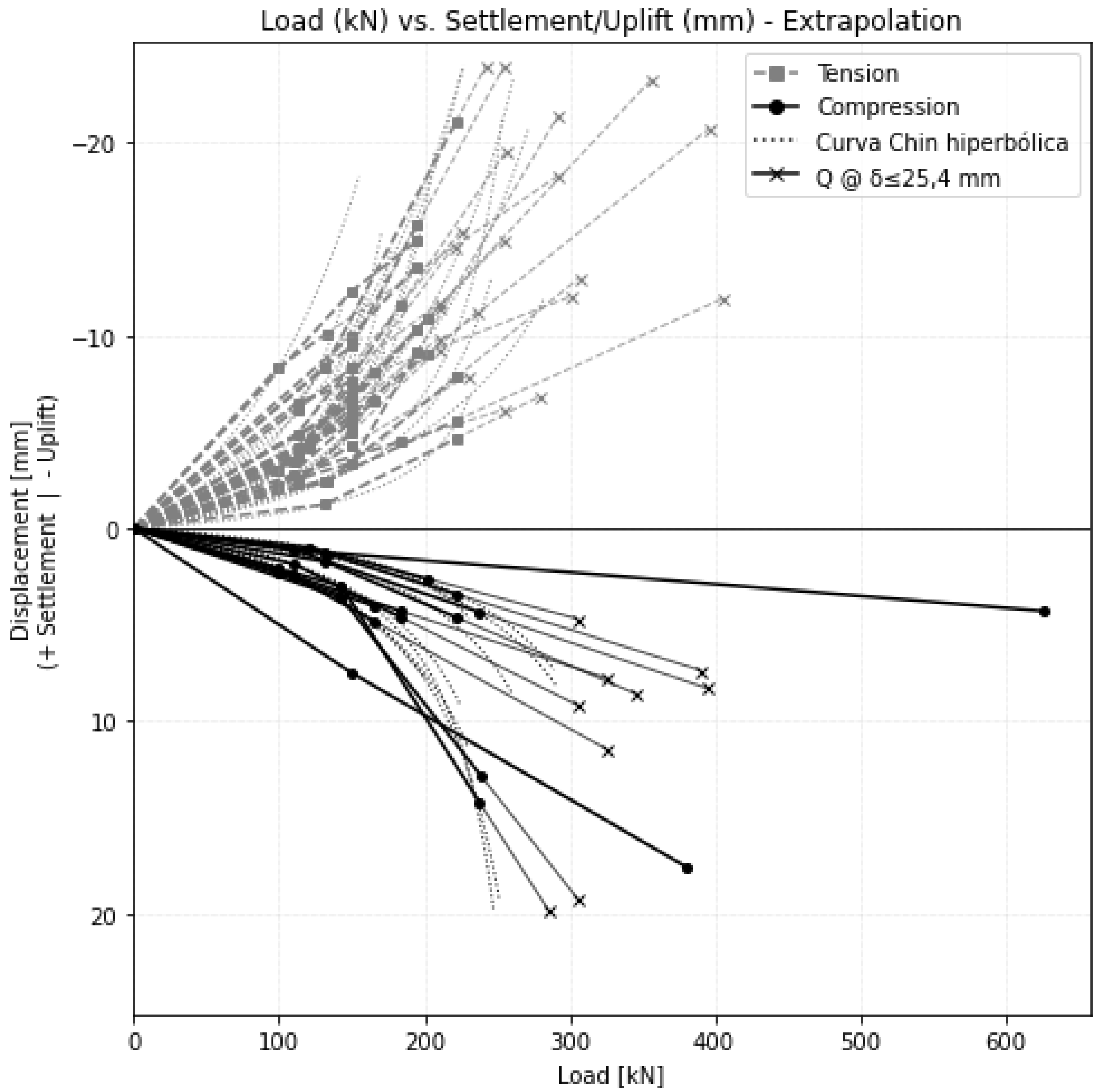

Figure 6. Load (kN) Vs Settlement/Uplift (mm) – Extrapolation

From the figure, two main aspects are important to mention. In one hand, in average the settlement or deformation for compression tests are inferior when comparing with the deformation for tension test. That result can lead to several conclusions such as the effect of the tip resistance for micropiles aspect that in the common practice is neglected. In the other hand, the ultimate load in general can range from 250 kN to 400 kN although the final load might be higher if the reference value of 25,4 mm is not considered as a potential failure point. Finally, from those values, a theorical distribution along micropiles is proposed based on the process described in the model framework.

Load test analyses

As mentioned, a total of 40 tests were conducted and analyzed. For the region studied only 2 tests reached failure which could be a clear limitation of the present study, even though an additional load test was included considering that it was conducted in a region with similar geotechnical conditions and similar design and construction conditions. Furthermore, other load tests reaching failure were analyzed with the purpose of validation, especially for extrapolation methods. Those additional tests are part of another study, and the geotechnical conditions differ considerably. It is important to mention that none of those tests are included in the graphs and calculations since they were part only for the extrapolation methods validation.

Now, regarding the type of micropiles tested and included in the present study, both type D and Hollow Bar micropiles were analyzed and extrapolated based on the methods validated. For some of those tests, the extrapolation process resulted in an unrealistic ultimate load, due to the method considerations. In those cases, the ultimate load was approximated to the response obtain for tests on micropiles with similar characteristics and settlement at the tested load.

It is important to note that the hollow bar micropiles tested were located at site 1 and IRS (Type D) micropiles were located at site 2. Other important aspects to consider include, on the one hand, that the load tests followed two different loading and unloading sequences (a single cycle and up to three load-unload cycles); and on the other hand, that the summary results of the tests were plotted considering only the design load and its associated settlement, as well as the test or failure load and its corresponding settlement. The overall results are summarized before in table [1] and illustrative behavior particularly comparing tension and compression test is shown before in figure 6. Additional information and comparisons are presented in the appendix.

Finally, from Figure 7 shown below, it is worth highlighting that the load–settlement curves show a relatively similar behavior between self-drilling micropiles (theoretically Type B or Type E) and predrilled micropiles (Type C or D), with generally lower average settlements observed in the self-drilling micropiles. This outcome may appear counterintuitive, considering that design tables and general practice typically associate higher bond strength values with Type C and Type D injection methods. This could be due to several factors, such as the construction techniques and installation equipment, but there is not enough information to conclude.

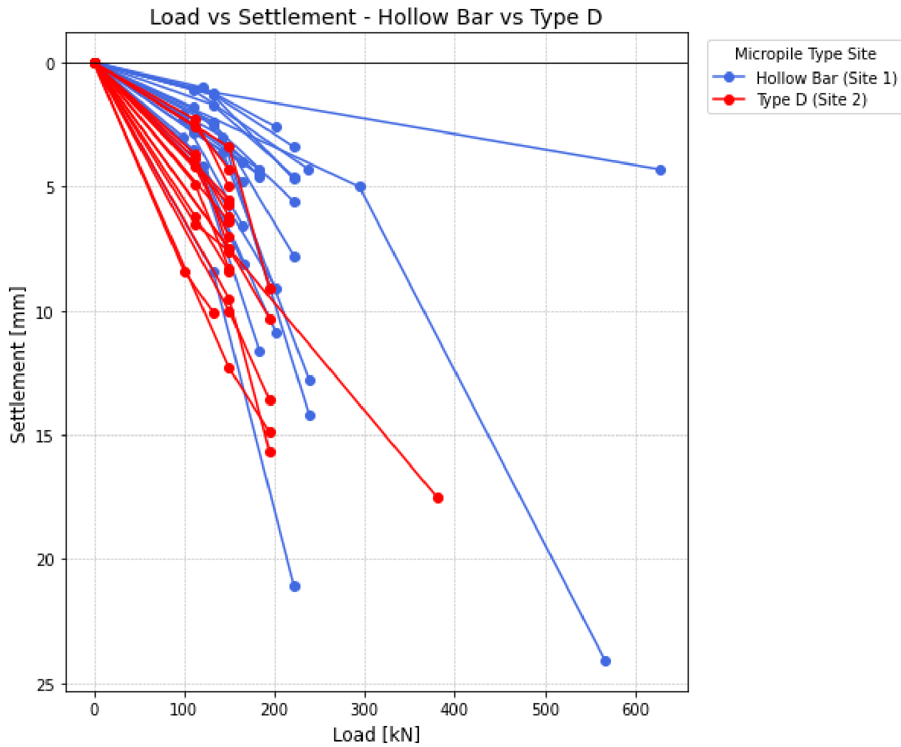

Figure 7. Load - Settlement comparison for hollow bar and Type D micropiles in tension vs compression

Model Development

This approach was applied using the average unit shaft resistance mobilized at the Test Load (TL) level for tension and compression load tests. The resulting estimates are summarized in the following figure for a particular case. The complete data regarding the distribution of the load transference along micropiles for each micropiles analyzed is presented as an appendix of the present work.

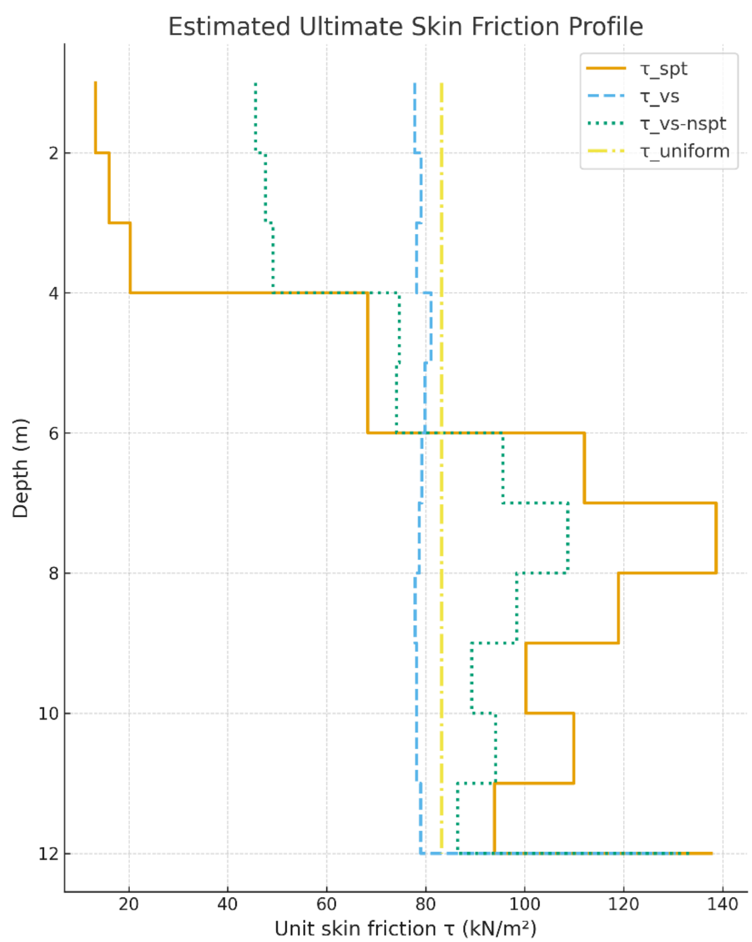

Figure 8. Skin friction per segment based on Vs and N-spt

Based on this initial estimation of unit skin friction along the micropile, a simple predictive model can be developed using field data such as the Standard Penetration Test (SPT) N-spt and shear wave velocity (Vs).

Thus, an initial approximation is proposed through a multiple linear regression model, as follows:

$$\tau = \beta_0 + \beta_1 \cdot N_{mean} + \beta_2 \cdot V_s$$

Where:

- τ: unit skin friction resistance (in kPa),
- N_{mean}: average SPT blow count,
- V_s: shear wave velocity (in m/s),
- *β0:* model intercept (baseline value),
- *β1,β2*: coefficients indicating how much τ changes per unit increase in *N* or V_s

Similarly, other simple regression models using N-SPT and Vs independently can also be developed, as well as more advanced machine learning models such as Random Forest. In any case, the quality and quantity of available data are critical to improving the predictive power of the models. Additionally, cross-validation should be performed to assess the models' predictive capabilities and to ensure the physical relevance of the input variables for both shear wave velocity (Vs) and standard penetration resistance (N-spt) that might have explanatory value in estimating unit skin friction resistance on micropiles.

In the case of the current model under development, the use of N-SPT and Vs values alone as input parameters to estimate a potential distribution of unit skin friction along the micropile, proportional to them, allows the building of preliminary predictions. These predictions can later be validated using additional load test data or available information from different sites with similar geotechnical environments.

Now, the development of the models is presented, as mentioned based on linear and multiple regression to estimate the influence of the independent variables (N-SPT and Vs) on the dependent variable, in this case τ. Predictive power, as well as the significance and the selection of the best model is presented.

Model multiple 1:

The initial multiple regression model, using shaft resistance distributed proportionally to N-SPT values, demonstrated a strong predictive power (Adjusted R^2 = 0.819). Both N-SPT and Vs were found to be statistically significant predictors, confirming that each variable provides valuable, non-redundant information for estimating shaft resistance.

$$\tau(\text{kPa}) = -20.62 + 2.05 \cdot N_{spt} + 0.09 \cdot V_s$$

Model Multiple 2:

When the shaft resistance was distributed proportionally to shear wave velocity, the resulting model also showed a robust correlation (Adjusted R^2 = 0.792). Again, both N-SPT and Vs proved to be highly significant variables, reinforcing the conclusion that a combined model is more comprehensive than one based on a single parameter.

$$\tau(\text{kPa}) = -16.27 + 2.64 \cdot N_{spt} + 0.11 \cdot V_s$$

Model Multiple 3:

This model, which used an averaged shaft resistance as the target variable, yielded the highest mathematical fit of all models (Adjusted R^2 = 0.871). An interesting outcome, however, is important to note that while N-SPT kept being extremely significant (p-value = 0.000), the Vs variable became statistically non-significant (p-value = 0.083). This suggests that the dominant predictive influence of N-SPT can limit the contribution of Vs in this combined format.

$$\tau(\text{kPa}) = -7.11 + 2.49 \cdot N_{spt} + 0.05 \cdot V_s$$

Model Simple 1:

The simple linear regression confirmed that N-SPT alone is an exceptionally strong predictor of skin friction resistance, with an Adjusted R^2 of 0.841, this model can account for 84.1% of the variability in τ, establishing N-SPT as the dominant predictive variable for this site.

$$\tau(\text{kPa}) = 5.23 + 2.39 \cdot N_{spt}$$

Model simple 2:

When analyzed independently, shear wave velocity was found to be a moderate predictor, explaining 53.3% of the variability in shaft resistance (Adjusted R^2 = 0.533). While statistically significant on its own, its predictive power is considerably lower than that of N-SPT.

$$\tau(\text{kPa}) = -52.49 + 0.54 \cdot V_s$$

The summary of the results for each model is presented in Table 3.

Table 3. Regression models

Model	Dependent Variable (tau)	Predictive Equation	Adjusted R2	p-value
Multiple 1	Tau, SPT based	tau = −20.62 + 2.05N_spt + 0.09V_s	0,819	Nspt: 0.000 & Vs: 0.003
Múltiple 2	Tau, Vs based	tau = −16.27 + 2.64N_spt + 0.11V_s	0,792	Nspt: 0.000 & Vs: 0.008
Múltiple 3	Tau, avg (SPT + Vs)	tau = −7.11 + 2.49N_spt + 0.05V_s	0,871	Nspt: 0.000 & Vs: 0.083
Simple 1	Tau, avg (SPT + Vs)	tau = 5.23 + 2.39N_spt	0,841	Nspt: 0.000
Simple 2	Tau, avg (SPT + Vs)	tau = −52.49 + 0.54V_s	0,533	Vs: 0.000

After evaluating all five models, the simple linear regression based only on N-SPT is recommended as the final predictive model. While the multiple regression using the averaged τ yielded the highest R-squared value, the lack of statistical significance for the Vs variable in that specific model makes it less robust from a theoretical point of view. The principle of parsimony suggests selecting the simplest model with the highest significant predictive power.

The simple N-SPT model is powerful, statistically significant, and explains a remarkable 84.1% of the variability.

Model Simple 1:

$$\boldsymbol{\tau(kPa) = 5.23 + 2.39 \cdot N_{spt}}$$

Finally, in the following figure the results are presented. In figure 8, the comparison between the actual and predicted bond resistance is shown, giving a better idea of the prediction power of the model selected.

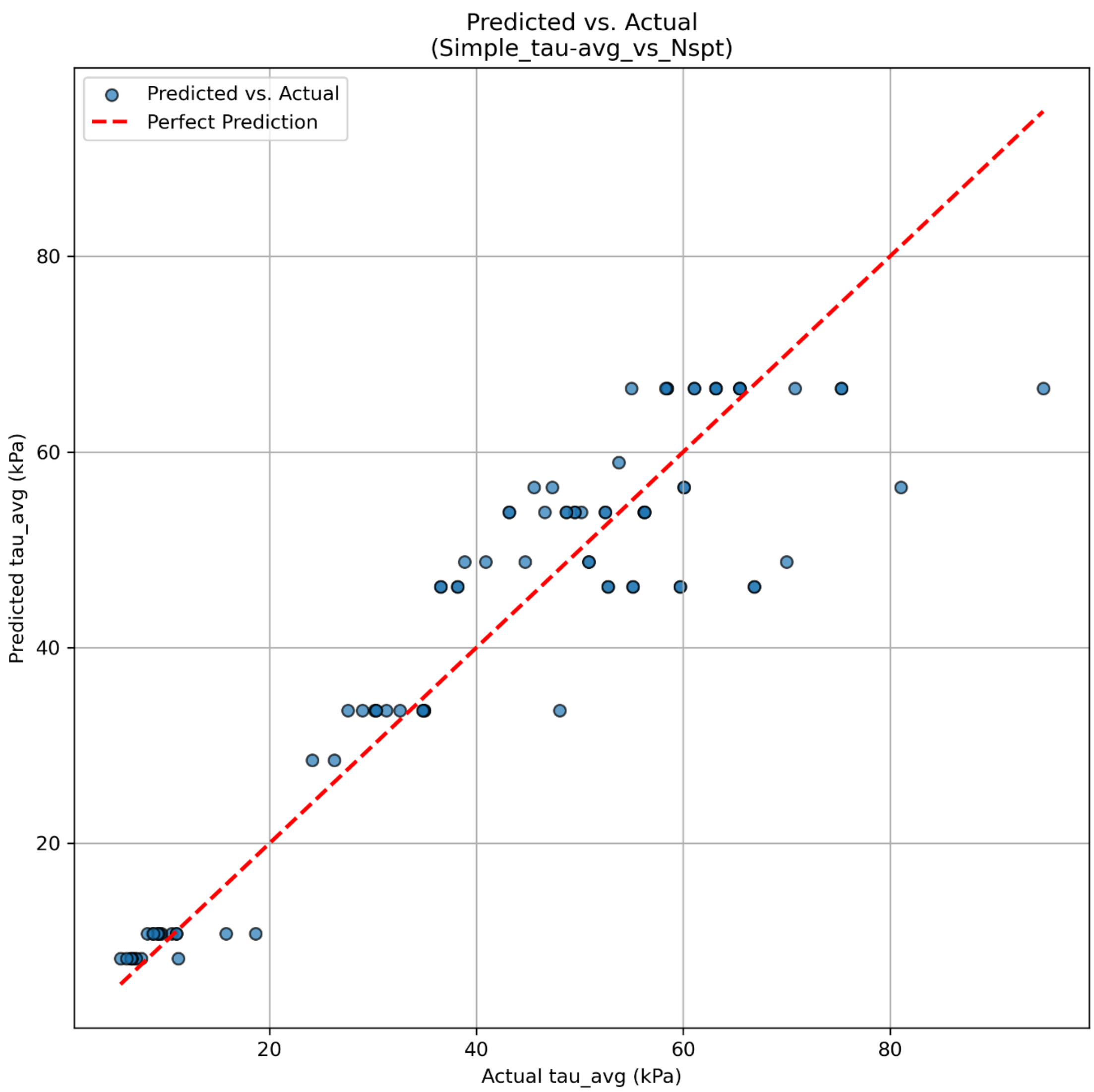

Figure 8. Predicted Vs Actual skin friction resistance, τ

As a final comment of the models evaluated, for the simple model 2 based only on Vs, it could be used as an initial prediction in those cases where information from SPT tests is not available or is not reliable, which are the cases for high energy alluvial soils with presence of boulders that can present difficulties for performing SPT. That preliminar estimation might be validated via site specific load tests.

Reliability approach and Resistance factors

This statistical approach is useful to determine the failure probability, and to propose a site geotechnical resistance factor being the based for LRFD or reliability analysis. This approach is also a key step to go from presumptive analysis and designs to predictive analysis with less uncertainty and therefore increasing the reliability and viability of micropiles projects as proposed by [2].

The design based on reliability implemented by LRFD is the framework to develop and calibrate resistance factors for geotechnical purposes. The main goal is to work with a specified target for the probability of failure considering the relationship between the uncertainties of skin friction resistance and the uncertainties of the applied loads. The LRFD design approach can be expressed as presented in the following equation:

$$\sum \eta_i Q_i \leq \phi R_n$$

Then, for the resistance factor the equation presented is considered based on [16]

$$\phi = \frac{\lambda_R \cdot \left(\gamma_D \frac{E[Q_D]}{E[Q_L]} + \gamma_L\right)}{\left(\frac{E[Q_D]}{E[Q_L]} + 1\right) \cdot \exp\left\{\beta_T \sqrt{Var[\ln R] + Var[\ln Q]}\right\}}$$

$\sum \eta_i Q_i$	Modified nominal load
R_n	Nominal Resistance
λ_R	Average resistance bias
ϕ	Resistance factor
σλ	Standard Deviation of bias
βT	Reliability Index
$COV\lambda$	Covariance of bias

The main objective of this chapter is to calibrate the site resistance factor for the predictive models proposed, especially those presented as Model Simple 1, and Model Multiple 3.

The calibration process is based on the Bayesian Inferences Method or as it is commonly known as the First Order of Second Moment Method (FOSM). Initially, the bias (λ) is quantified as well as the Covariance of the predictive model. In the following equation, the bias is defined as the relationship between the skin friction obtained from load tests records and the skin friction predicted with the equations from the regression models proposed. It is important to note that for the models proposed, several assumptions were made considering the lack of information from tests reaching failure and the necessity of extrapolating most of the data obtained from tests.

$$\lambda = \frac{\tau_{actual}}{\tau_{nominal}}$$

Where:

τ_{actual}: Is the value of the skin friction resistance obtained from the predictive model

$\tau_{nominal}$: Is the value of the skin friction resistance obtained from the 40 load tests performed.

Note: To consider the differences in geotechnical condition in depth, the skin friction per meter was obtained assigning the resistance proportional to SPT or Vs for each meter.

The models proposed have shown a high determination coefficient with an adjusted R^2 of 0,841 for the Model Simple 1, and 0,871 for the model Multiple 3. For those models, based on the results the uncertainty of the model is low, and the bias is in general close to 1.

Factor Resistance Proposal

In general, the literature of LRFD methods suggests that well validated predictive methods can consider resistance factors higher than the ones considered for presumptive methods as presented in [3], those predictive models can obtain factors ranging from 0,6 to 0,9 or even 1 depending on the quality and quantity of data. For the present calibration of the resistance factor for the models analyzed the following process was carried out to estimate the factor.

First, the resistance bias and average bias for the unit skin resistance are calculated as follows.

$$\lambda_i = \frac{\tau_{actual,i}}{\tau_{nominal,i}}$$

$$\lambda_R = \frac{1}{N}\sum_{i=1}^{N}\lambda_i$$

Then, the standard deviation and covariance for load and resistance are calculated

$$\sigma_\lambda = \sqrt{\frac{1}{N-1}\sum_{i=1}^{N}(\lambda_i - \lambda_R)^2}$$

$$COV_R = \frac{\sigma_\lambda}{\lambda_R}$$

$$COV_Q = \frac{\sqrt{E[Q_D]^2 \cdot COV_{Q_D}^2 + E[Q_L]^2 \cdot COV_{Q_L}^2}}{E[Q_D] + E[Q_L]}$$

And finally, the reliability index (βT) is selected ranging from 2 to 3, with 2,33 the common practice value for geotechnical applications. That aims to an implicit probability of failure of 1% for normal and log-normal distribution. Additionally, it is important to note that the load factors $\gamma_D = 1{,}25$ (for dead load) and $\gamma_L = 1{,}75$ (for the live load) are defined based on the AASHTO recommendation.

$$\phi = \frac{\lambda_R \cdot \left(\gamma_D \frac{E[Q_D]}{E[Q_L]} + \gamma_L\right)}{\left(\frac{E[Q_D]}{E[Q_L]} + 1\right) \cdot \exp\left\{\beta_T \sqrt{Var[\ln R] + Var[\ln Q]}\right\}}$$

Now, to illustrate the variation of the Resistance Factor with Beta, is shown in table 4.

Table 4. Resistance Factor & Failure Probability

Reliability Index (βT)	**Failure Probability (Pf)**	**Resistance Factor (ϕ)**
2	2.3%	0,76
2,1	1.8%	0,73
2,2	1.4%	0,71
2,3	1.1%	0,69
2,33	1.0%	0,68
2,4	0.8%	0,67
2,5	0.6%	0,65
2,6	0.5%	0,63
2,7	0.3%	0,61
2,8	0.3%	0,59
2,9	0.2%	0,57
3	0.1%	0,55

Then, the value proposed as a factor resistance associated with the models evaluated is $\phi = 0{,}68$ for a probability of failure of 1%.

Validation and comparison with existing methods

To validate predictions of the model selected based only on N-spt (Model Simple 1), a comparison was established using benchmark estimations based on FHWA recommended values for soils with similar characteristics. Considering that the values from FHWA correspond to a wide range of values for each combination of soils and injection type, several values were included to estimate the maximum, minimum and average values accounting for changes in the ground to grout resistance (τ or α_{bond}) along the micropiles being strongly dependent on the personal criteria of the designer. Once these boundaries were established, a comparison was proposed for the estimation with the predictive model selected for different resistance factors for those cases where LRFD is considered, and safety factors (FS = 2) where ASD is considered. In figure 9, those cases are illustrated.

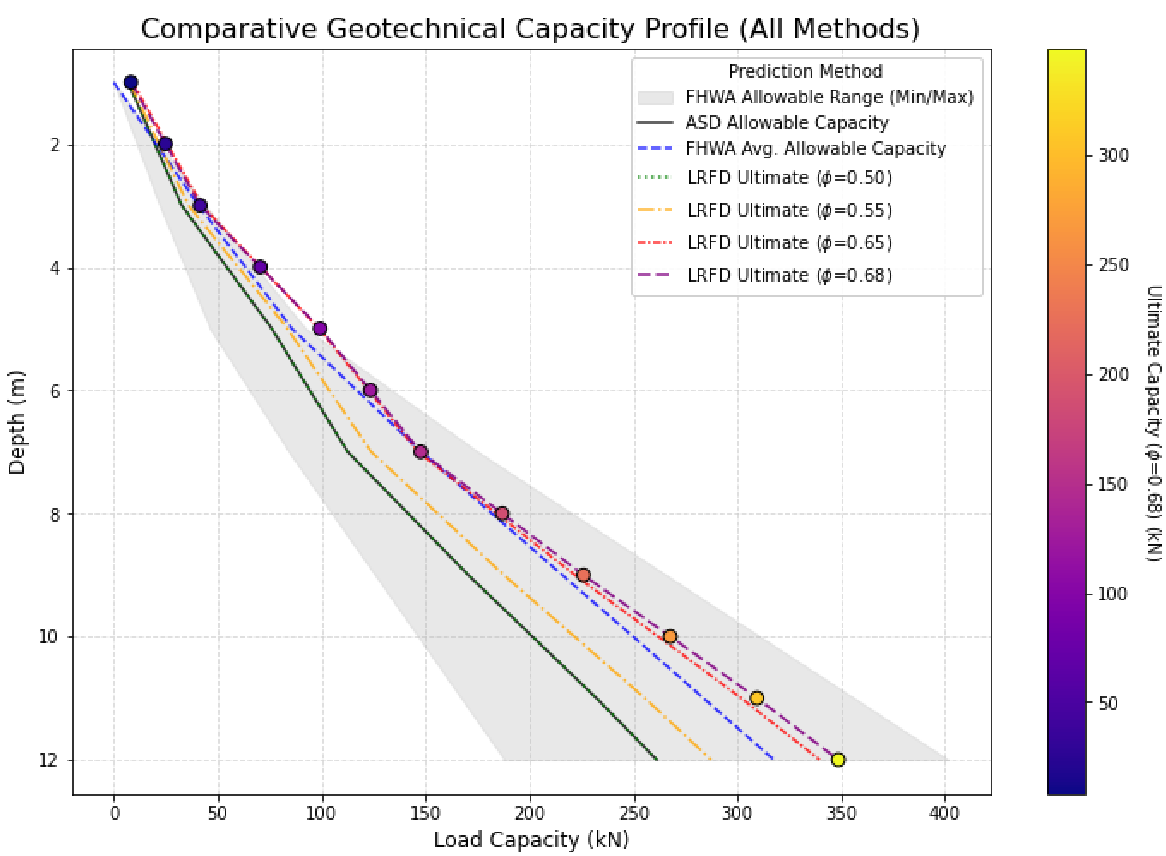

Figure 9. Geotechnical resistance comparison

Limitations of the study

Beyond the limitations already mentioned related with the limited number of tests reaching failure, the absence of instrumented micropiles with strain gauges, hence the necessity of used extrapolation methods and proposed methods to distribute load along micropiles bring uncertainties that can be addressed by implementing an even more robust load testing plan, including instrumentation and more information to failure.

The models presented in this study, product of the regression processes, were solely validated for soils with the characteristics where the tests were performed. Then, its applicability is limited to fine granular soils, medium alluvial material as described. Then, it is not appropriate to coarse soils, gravel and high energy alluvial material. For those purposes, different models should be implemented.

Finally, additional analysis can be done, to better understand and characterize the inherent differences in the grout to ground bond resistance due to differences in the construction process, not only with the variation of the injection methods but also those differences related to injection pressure, grout consumption, expertise of the personal involved in the construction and the equipment and technics used for the drilling. In general, micropiles are dependent on various factors including those from the construction stage.

Conclusions

- The statistical and predictive power of the models depends on the quantity and quality of the available data; therefore, standardization of load tests, as well as failure criteria and their subsequent analysis, is crucial. Additionally, understanding potential differences in the geotechnical behavior of micropiles depending on the construction procedure or injection type is key for analyses, especially when comparing the results obtained from load tests with various geotechnical design methods for micropiles.
- The lack of detailed information from load tests reaching failure and from instrumented micropiles to estimate load distribution along micropiles is a challenge that many projects face in common practice. As shown in the present work, a framework to deal with those constraints can enhance the way projects involving micropiles are planned and developed.
- Regression models are still a useful tool to estimate the behavior of certain variables when associated parameter varies. As presented, the results from the regression models assessed in this work can lead to a more particular value of ground to grout resistance, being a complementary method for FHWA ranges that usually lead to a conservative design.
- The initial multiple regression model, using skin friction resistance distributed proportionally to N-SPT values, demonstrated a strong predictive power (Adjusted $R^2 = 0.819$). Both N-SPT and Vs were found to be statistically significant predictors, confirming that each variable provides valuable, non-redundant information for estimating shaft resistance.
- A key finding of the regression analysis is the comparatively low statistical significance of shear wave velocity (Vs) as a predictor for ultimate shaft resistance, especially when N-SPT data is included. This can be attributed to two primary factors:
    - Low-Strain Measurement vs. High-Strain Failure: Shear wave velocity is fundamentally a low-strain soil parameter, measuring stiffness at deformations that are orders of magnitude smaller than those required to mobilize ultimate shaft resistance. As the micropile approaches failure, the soil enters a high-strain, plastic state where its behavior is no longer governed by the initial stiffness that Vs effectively measures.

- Inherent Variability and Interpretation: The acquisition and interpretation of Vs data, particularly in stratified alluvial deposits, can introduce significant variability. Factors such as the testing method, signal processing, and layer interpretation can lead to a wide range of values, reducing the precision of Vs as a direct input for a predictive model and diminishing its statistical significance.

Despite this finding, the model based on the simple regression for Vs, can still be useful for preliminary designs and verifications when access to geotechnical information is limited.

- After evaluating all five models, the simple linear regression based only on N-SPT is recommended as the final predictive model. While the multiple regression using the averaged τ yielded the highest R-squared value, the lack of statistical significance for the Vs variable in that specific model makes it less robust from a theoretical point of view. The principle of parsimony suggests selecting the simplest model with the highest significant predictive power. The simple N-SPT model is powerful, statistically significant, and explains a remarkable 84.1% of the variability.
- Initially, multiple linear regression models incorporating both N-SPT and Vs were developed to investigate the combined influence of these parameters. While these models yielded a high coefficient of determination, the analysis revealed that the contribution of Vs was not statistically significant in the presence of N-SPT. This finding led to the evaluation of simpler, more robust models.
- The strength of this model lies in its developmental framework, which is designed for continuous updating. It can be progressively refined by incorporating new data from load tests to failure, instrumented piles, or by including new variables that influence shaft resistance.
- The progressive validation revealed a critical inflection point in the predictive models. At a deformation of approximately 10 mm, the reliability of the hyperbolic methods (Chin and Decourt) begins to decrease. Beyond this threshold, their predictions started to diverge significantly from the measured performance, consistently overestimating the ultimate capacity. This finding suggests a practical limit to their applicability; while these methods are robust for modeling behavior at moderate strains, their underlying hyperbolic assumption loses fidelity as the micropiles approaches an advanced failure state where more complex soil mechanics govern the response.

- Based on the test results conducted on two types of micropiles: predrilled micropiles with Type C or D grout injection (16 tests) and self-drilling hollow bar micropiles with Type B injection (24 tests) no significant differences in performance were observed. Both types exhibited similar deformation values under comparable load levels. This outcome may differ slightly from commonly recommended soil–grout bond values, where higher values are typically suggested for Type C or D injection compared to Type B. However, such differences may be attributed to specific installation conditions, pumping systems, and other influencing factors.
- The predictive and load-test-based design approaches proposed in [4] may yield reliable results, allowing for accurate estimation of bond factors and unit skin friction resistance in micropiles. This enables the application of higher resistance factors, leading to more cost-effective designs.
- To accurately determine the unit skin friction distribution along micropiles and to develop reliable predictive models, instrumentation and numerical modeling play a fundamental role. Consequently, the next steps in this research project aim to implement both techniques.
- The possibility of gathering more load test data that reach failure, or alternatively, applying robust extrapolation techniques to estimate the failure load of micropiles tested only up to a service or test load, opens significant opportunities for analysis and the development of reliable predictive models.
- The lack of instrumentation, limited data, and insufficient geotechnical characterization of the tested soils impose constraints on the proposed models and emphasize the need for validation. Therefore, the estimated values suggested here should be regarded as guidelines and preliminary approximations.
- Based on the available information, it is feasible to incorporate analyses that consider the settlement levels reached at various loading stages, which in turn enables the development of tools for predicting settlements in micropiles.
- When comparing the predictions with the selected model, is important to note that for each case analyzed (for different resistance factors), and for those cases for ASD with safety factor (FS=2), the values obtained are always between the limits established with the minimum and maximum values from FHWA, with values for resistance factor ϕ=0,65; higher than the average values obtained using FHWA. These results are a good benchmark for understanding the predictive and uncertainty level of the model proposed.

- Additional analyses are needed, especially with more information from load tests reaching failure and instrumented micropiles to improve the reliability of the model and the capacity to estimate more accurately the load transfer along the micropiles increasing the capabilities for the decision-making process after getting information from the load testing program.

Future work

- As proposed future works on bond resistance on micropiles, studies that include more information from failure tests and instrumented micropiles can be crucial to enhance the understanding of micropiles behavior and their load distribution along the shaft.
- Other predictive methods can be developed for coarse soils, gravel and high energy alluvial environments where conventional field tests such as N-spt are not reliable or even applicable.
- Research on tip resistance on micropiles is interesting considering the results obtained when comparing settlements obtained in compression and tension tests that might indicate effects of tips resistance on settlements.
- Generative models can be used to predict and calibrate designs due to the information that can be collected from the micropile projects in different regions.
- Numerical modelling to investigate the load transfer along micropiles can be implemented. Allowing designers a better understanding and decision-making to optimized micropiles projects.

References

- [1] P. J. Sabatini, B. Tanyu, T. Armour, P. Groneck, and J. Keeley, *Micropile Design and Construction: Reference Manual for NHI Course No. 132078*, FHWA NHI-05-039. Washington, DC: U.S. Department of Transportation, Federal Highway Administration, Dec. 2005.

- [2] J. E. Loehr, A. Z. Boeckmann, and D. D. Ding*, Reliability-Based Geotechnical Resistance Factors for Axially Loaded Micropiles.* Washington, DC: The National Academies Press, 2022. Disponible en: https://doi.org/10.17226/26615

- [3] M. Bustamante and B. Doix, *Une méthode pour le calcul des tirants et des micropieux injectés*. Paris: Laboratoire Central des Ponts et Chaussées, 1985.

- [4] H. Zhang, Y. Wang, y Z. Liu*, "Improved α- and β-Methods for the Estimation of Shaft Resistance of Driven Piles in Intermediate Geomaterials,"* en Geo-Congress 2020: Foundations, Soil Improvement, and Erosion Control, Reston, VA: American Society of Civil Engineers, 2020, pp. 112–121

- [5] M. N. Elsiragy, "Comparative Investigation of Loading Test on Micro-Piles Installed with Different Technique – (Case Study)," *Eur. J. Eng. Technol. Res.*, vol. 6, no. 4, pp. 89–97, Jun. 2021. [En línea]. Disponible en: **https://www.ej-eng.org/index.php/ejeng/article/view/2454**

- [6] M. Elkasabgy, "Finite Element Analysis of the Axial Capacity of Micropile," in *Proc. 8th Int. Workshop on Micropiles*, Toronto, Canada, 2007, pp. 1–12. [En línea]. Disponible en: **https://www.ismicropiles.org/Proceedings/2007/Elkasabgy%20-%20Paper%20FE%20Analysis%20of%20Axial%20Capacity%20of%20Micropiles.pdf**

- [7] A. Y. Abd Elaziz and M. H. El Naggar, "Geotechnical Capacity of Hollow-Bar Micropiles in Cohesive Soils," *Can. Geotech. J.*, vol. 51, no. 10, pp. 1123–1138, 2014.

- [8] A. Misra, C.-H. Chen, R. Oberoi, and A. Kleiber, "Simplified Analysis Method for Micropiles Pullout Behavior," *J. Geotech. Geoenviron. Eng.*, vol. 130, no. 10, pp. 1024–1033, Oct. 2004. [En línea]. Disponible en: https://ascelibrary.org/doi/10.1061/(ASCE)1090-0241(2004)130:10(1024)

- [9] T. M. Allen, *Development of Geotechnical Resistance Factors and Downdrag Load Factors for LRFD Foundation Strength Limit State Design*, FHWA-NHI-05-052. Washington, DC: U.S. Department of Transportation, Federal Highway Administration, 2005.

- [10] G. A. Fenton and D. V. Griffiths, "Geotechnical resistance factors for ultimate limit state design of deep foundations in frictional soils," *Can. Geotech. J.*, vol. 48, no. 1, pp. 114–124, Jan. 2011. [En línea]. Disponible en: https://doi.org/10.1139/t11-068

- [11] X. Yang, J. Han, and R. L. Parsons, *Development of Recommended Resistance Factors for Drilled Shafts in Weak Rocks Based on O-Cell Tests*. Lawrence, KS: University of Kansas; Topeka, KS: Kansas Department of Transportation, Mar. 2010. [En línea]. Disponible en: https://rosap.ntl.bts.gov/view/dot/27783

- [12] F. K. Chin, "Estimation of the Ultimate Load of Piles from Tests Not Carried to Failure," in *Proc. 2nd Southeast Asian Conf. Soil Eng.*, Singapore, 1970, pp. 81–92. [En línea]. Disponible en: **https://www.scribd.com/document/576695076/Estimation-of-the-Ultimate-Load-of-Piles-from-Tests-not-Carried-to-Failu**

- [13] L. Decourt, "Análise de resultados de provas de carga em estacas," in *Anais do 10º Congresso Brasileiro de Mecânica dos Solos e Engenharia Geotécnica*, vol. 2, Foz do Iguaçu, Brasil, 1995, pp. 685–692.

- [14] C. Van der Veen, "The bearing capacity of a pile," in *Proc. 3rd Int. Conf. Soil Mech. Found. Eng.*, Zurich, Switzerland, Aug. 1953, vol. 2, pp. 84–90.

- [15] J. Brinch Hansen, "Discussion on hyperbolic stress-strain response, cohesive soils," J. Soil Mech. and Found. Div., ASCE, vol. 89, no. SM4, pp. 241-242, Jul. 1963

- [16] H. D. Butler and H. E. Hoy, *Users Manual for the Texas Quick-Load Method for Foundation Load Testing*. Washington, DC, USA: Federal Highway Administration, U.S. Dept. of Transportation, Rep. FHWA-IP-77-8, 1977.

- [17] D. G. Fredlund, H. Rahardjo, y M. D. Fredlund, Unsaturated Soil Mechanics in Engineering Practice, Hoboken, NJ: John Wiley & Sons, 2012.

- [18] G. B. Baecher y J. T. Christian, "Chapter 18: Load and Resistance Factor Design," en *Reliability and Statistics in Geotechnical Engineering*. Chichester, New York: John Wiley & Sons, 2003.

Appendix A | Micropiles Data Collection

Site	Micropile Type	MP#	Test Type	D [mm]	L [m]	Design Load, DL [kN]	Test Load,TL [kN]	Settlement at DL [mm]	Settlement at TL [mm]	Failure?
1	HollowBar	MP1	Tension	200,0	12,8	132,0	222,0	2,5	5,6	No
1	HollowBar	MP2	Compression	200,0	12,8	132,0	222,0	1,7	4,6	No
1	HollowBar	MP3	Tension	200,0	11,8	132,0	222,0	8,4	21,1	No
1	HollowBar	MP4	Compression	200,0	13,8	143,0	238,8	3,6	12,8	No
1	HollowBar	MP5	Compression	200,0	12,8	143,0	238,0	3,0	14,2	No
1	HollowBar	MP6	Tension	200,0	9,8	99,1	165,5	3,0	8,1	No
1	HollowBar	MP7	Tension	200,0	12,8	132,0	222,0	1,3	4,7	No
1	HollowBar	MP8	Compression	200,0	10,8	110,0	238,0	1,1	4,3	No
1	HollowBar	MP9	Compression	200,0	10,8	110,0	183,7	1,8	4,6	No
1	HollowBar	MP10	Tension	200,0	10,8	110,0	183,7	3,5	11,6	No
1	HollowBar	MP11	Compression	200,0	9,8	99,0	165,3	2,3	4,0	No
1	HollowBar	MP12	Compression	200,0	9,8	99,0	165,3	2,1	4,8	No
1	HollowBar	MP13	Compression	200,0	10,8	110,0	183,7	2,5	4,3	No
1	HollowBar	MP14	Compression	200,0	11,8	121,0	202,1	1,0	2,6	No
1	HollowBar	MP15	Compression	200,0	12,8	133,0	222,1	1,3	3,4	No
1	HollowBar	MP16	Tension	200,0	11,8	121,0	202,1	4,2	9,1	No
1	HollowBar	MP17	Tension	200,0	9,8	99,0	165,3	2,2	6,6	No
1	HollowBar	MP18	Tension	200,0	12,8	133,0	222,1	2,4	7,8	No
1	HollowBar	MP19	Tension	200,0	11,8	121,0	202,1	4,4	10,9	No
1	HollowBar	MP20	Tension	200,0	10,8	110,0	183,7	2,8	4,5	No
1	HollowBar	MP21	Compression	200,0	12,0	132,0	627,0	1,2	17,0	Si
2	Type D	MP1	Tension	200,0	11,0	150,0	150,0	5,5	5,5	No
2	Type D	MP2	Tension	200,0	11,0	150,0	150,0	6,4	6,4	No
2	Type D	MP3	Tension	200,0	11,0	150,0	150,0	5,7	5,7	No
2	Type D	MP4	Tension	200,0	11,0	150,0	195,0	12,3	14,9	No
2	Type D	MP5	Tension	200,0	11,0	150,0	195,0	6,5	10,3	No
2	Type D	MP6	Compression	200,0	11,0	150,0	380,0	7,5	17,5	Si
2	Type D	MP7	Tension	150,0	10,0	150,0	195,0	10,0	13,6	No
2	Type D	MP8	Tension	150,0	10,0	150,0	195,0	3,4	9,1	No
2	Type D	MP9	Tension	150,0	10,0	150,0	195,0	9,5	15,7	No
2	Type D	MP10	Tension	150,0	10,0	100,0	133,0	8,4	10,1	No
2	Type D	MP11	Tension	200,0	11,0	112,5	150,0	6,5	7,6	No
2	Type D	MP12	Tension	200,0	11,0	112,5	150,0	3,7	7,5	No
2	Type D	MP13	Tension	200,0	11,0	112,5	150,0	4,2	7,0	No
2	Type D	MP14	Tension	200,0	11,0	112,5	150,0	2,3	5,0	No
2	Type D	MP15	Tension	200,0	11,0	112,5	150,0	3,9	6,2	No
2	Type D	MP16	Tension	200,0	11,0	112,5	150,0	6,2	8,3	No
2	Type D	MP17	Tension	200,0	11,0	112,5	150,0	4,9	8,4	No
2	Type D	MP18	Tension	200,0	11,0	112,5	150,0	2,6	4,3	No
4	HollowBar	MP1	Compression	150,0	12,0	280,0	570,0	5,0	24,0	Si

Category	Sub.Category	Quantity	Max Settlement at DL [mm]	Max Settlement at TL [mm]	Diameter range (mm)	Lenght range (m)
Test Type	Compression Tests	13	5	24	150 - 200	10 to 12
Test Type	Tension Tests	27	9	15,7	150 - 200	10 to 12
Micropile Type	Hollow Bar	22	5	24	150 - 200	10 to 12
Micropile Type	Type D	18	9,5	15,7	150 - 200	10 to 12
Performance	Tests to Failure	3	9,5	24	150 - 200	10 to 12
Performance	Non-Failure Tests	37	9	15,7	150 - 200	10 to 12
Performance	Total Load Tests	40	9,5	24	150 - 200	10 to 12

Appendix B | Micropiles Comparisons a Load Test Behavior

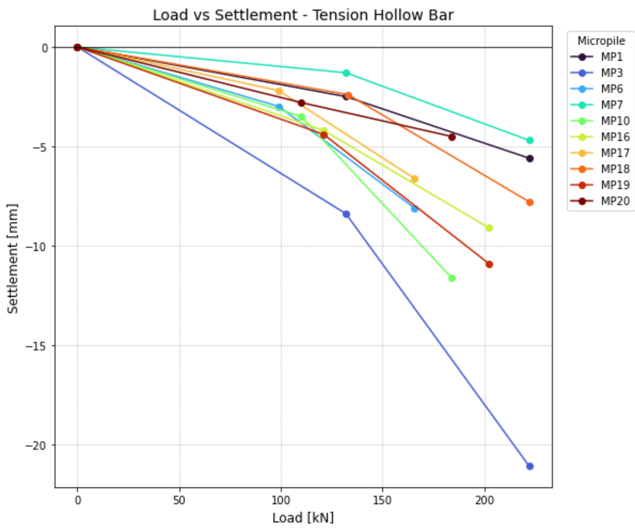

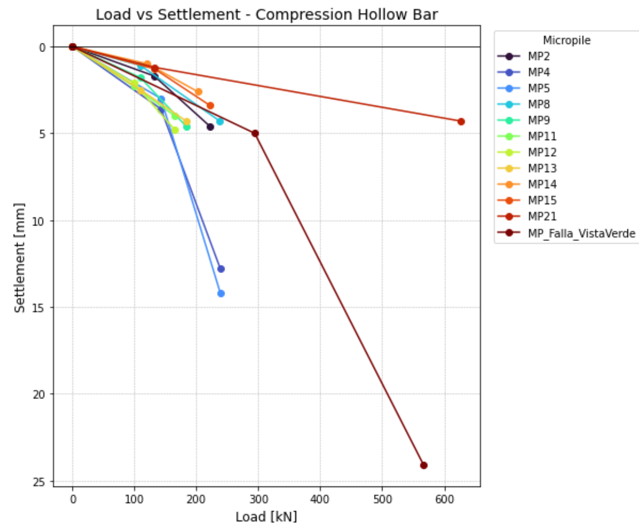

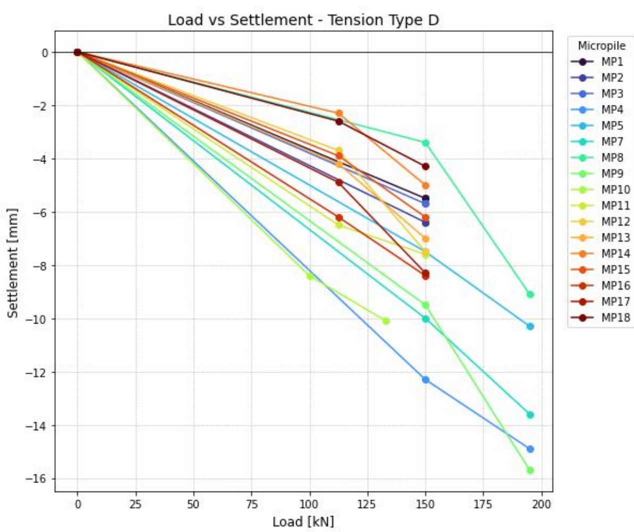

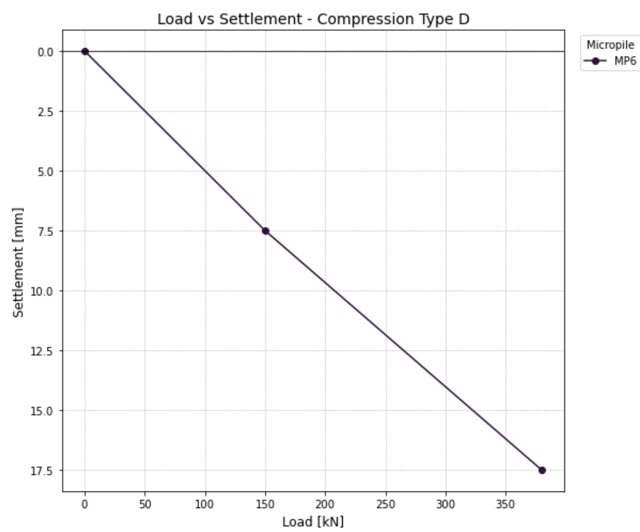

In total, only 2 out of 40 tests reached failure, both of which occurred under compression. Additionally, based on observations from the test that reached failure at Site 2 (Type D micropiles), it is presumed that the failure was due to buckling of the micropile within the upper meters, likely caused by insufficient head reinforcement. Finally, the figures present a comparison of the load–settlement curves between hollow bar micropiles and Type D micropiles.

Appendix C | Unit Skin Friction Model for the Data Set of Micropiles

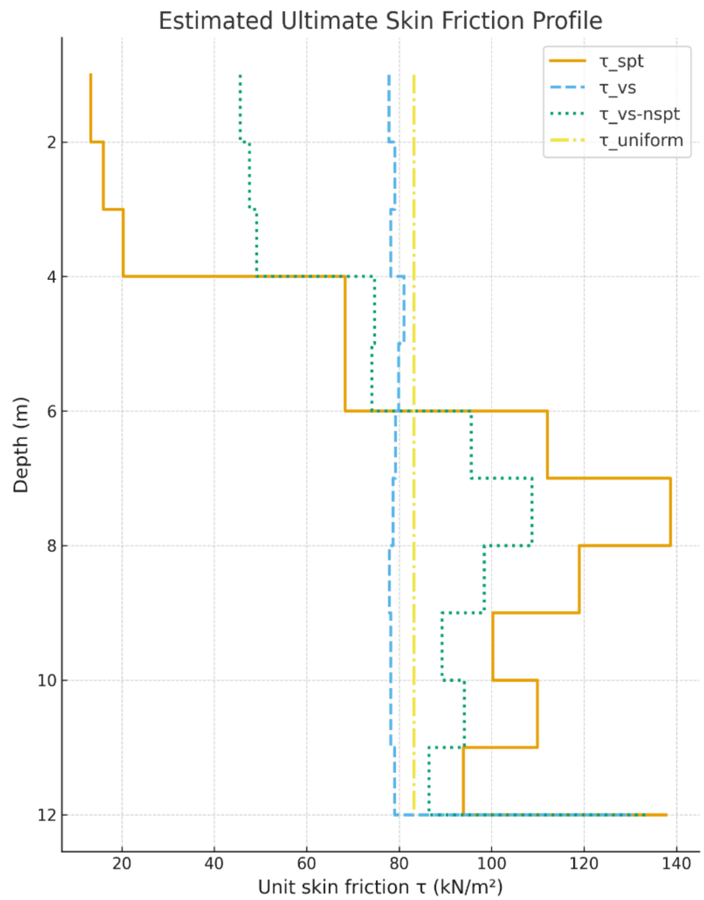

	Analysis Segment	Nspt, avg	Shear Wave Vel, Vs_avg [m/s]	Shear Strenght at Qu [kN/m2]	Nspt_i/ΣNspt	Ti (spt) [kN/m2]	Vs_i/ΣVs	Ti_(Vs) [kN/m2]	Ti_(Vs-Nspt) [kN/m2]	Analysis Segment	N _ Mean/m	Shear Wave Vel (VS)_Mean [m/s]	Ti_spt (kN/m2)	Ti_Vs (kN/m2)	Ti_Vs-Nspt (kN/m2)
	Segmento 1, Micropilote 1	3	156	43,0	0,01	6,9	0,1	40,2	23,6	Segmento 1, Micropilote 1	3	156	6,9	40,2	23,6
	Segmento 2, Micropilote 1	3	159	43,0	0,02	8,3	0,1	40,9	24,6	Segmento 2, Micropilote 1	3	159	8,3	40,9	24,6
	Segmento 3, Micropilote 1	4	157	43,0	0,02	10,5	0,1	40,5	25,5	Segmento 3, Micropilote 1	4	157	10,5	40,5	25,5
	Segmento 4, Micropilote 1	13	163	43,0	0,07	35,3	0,1	42,0	38,6	Segmento 4, Micropilote 1	13	163	35,3	42,0	38,6
	Segmento 5, Micropilote 1	13	160	43,0	0,07	35,3	0,1	41,3	38,3	Segmento 5, Micropilote 1	13	160	35,3	41,3	38,3
1	Segmento 6, Micropilote 1	21	159	43,0	0,11	58,0	0,1	41,0	49,5	Segmento 6, Micropilote 1	21	159	58,0	41,0	49,5
	Segmento 7, Micropilote 1	26	158	43,0	0,14	71,8	0,1	40,7	56,2	Segmento 7, Micropilote 1	26	158	71,8	40,7	56,2
	Segmento 8, Micropilote 1	22	156	43,0	0,12	61,6	0,1	40,3	50,9	Segmento 8, Micropilote 1	22	156	61,6	40,3	50,9
	Segmento 9, Micropilote 1	19	157	43,0	0,10	51,9	0,1	40,5	46,2	Segmento 9, Micropilote 1	19	157	51,9	40,5	46,2
	Segmento 10, Micropilote 1	21	157	43,0	0,11	56,9	0,1	40,5	48,7	Segmento 10, Micropilote 1	21	157	56,9	40,5	48,7
	Segmento 11, Micropilote 1	18	159	43,0	0,09	48,6	0,1	40,9	44,7	Segmento 11, Micropilote 1	18	159	48,6	40,9	44,7
	Segmento 12, Micropilote 1	26	262	43,0	0,14	71,2	0,1	67,5	69,4	Segmento 12, Micropilote 1	26	262	71,2	67,5	69,4
	Segmento 1, Micropilote 2	3	156	49,9	0,0	8,0	0,1	46,6		Segmento 1, Micropilote 2	3	156	8,0	46,6	27,3
	Segmento 2, Micropilote 2	3	159	49,9	0,0	9,6	0,1	47,5		Segmento 2, Micropilote 2	3	159	9,6	47,5	28,5
	Segmento 3, Micropilote 2	4	157	49,9	0,0	12,2	0,1	46,9		Segmento 3, Micropilote 2	4	157	12,2	46,9	29,5
	Segmento 4, Micropilote 2	13	163	49,9	0,1	41,0	0,1	48,6		Segmento 4, Micropilote 2	13	163	41,0	48,6	44,8
	Segmento 5, Micropilote 2	13	160	49,9	0,1	41,0	0,1	47,9		Segmento 5, Micropilote 2	13	160	41,0	47,9	44,4
2	Segmento 6, Micropilote 2	21	159	49,9	0,1	67,2	0,1	47,5		Segmento 6, Micropilote 2	21	159	67,2	47,5	57,4
	Segmento 7, Micropilote 2	26	158	49,9	0,1	83,2	0,1	47,2		Segmento 7, Micropilote 2	26	158	83,2	47,2	65,2
	Segmento 8, Micropilote 2	22	156	49,9	0,1	71,4	0,1	46,7		Segmento 8, Micropilote 2	22	156	71,4	46,7	59,0
	Segmento 9, Micropilote 2	19	157	49,9	0,1	60,2	0,1	46,9		Segmento 9, Micropilote 2	19	157	60,2	46,9	53,6
	Segmento 10, Micropilote 2	21	157	49,9	0,1	65,9	0,1	46,9		Segmento 10, Micropilote 2	21	157	65,9	46,9	56,4
	Segmento 11, Micropilote 2	18	159	49,9	0,1	56,3	0,1	47,4		Segmento 11, Micropilote 2	18	159	56,3	47,4	51,9
	Segmento 12, Micropilote 2	26	262	49,9	0,1	82,6	0,1	78,3		Segmento 12, Micropilote 2	26	262	82,6	78,3	80,4

	Analysis Segment	Nspt, avg	Shear Wave Vel, Vs_avg [m/s]	Shear Strenght at Qu [kN/m2]	Nspt_i/ΣN spt	Ti (spt) [kN/m2]	Vs_i/ΣVs	Ti_(Vs) [kN/m2]	Ti_(Vs-Nspt) [kN/m2]	Analysis Segment	N _ Mean/m	Shear Wave Vel (VS)_Mean [m/s]	Ti_spt (kN/m2)	Ti_Vs (kN/m2)	Ti_Vs-Nspt (kN/m2)
	Segmento 1, Micropilote 3	3	156	35,2	0,0	5,6	0,1	32,9		Segmento 1, Micropilote 3	3	156	5,6	32,9	19,3
	Segmento 2, Micropilote 3	3	159	35,2	0,0	6,8	0,1	33,5		Segmento 2, Micropilote 3	3	159	6,8	33,5	20,1
	Segmento 3, Micropilote 3	4	157	35,2	0,0	8,6	0,1	33,1		Segmento 3, Micropilote 3	4	157	8,6	33,1	20,8
	Segmento 4, Micropilote 3	13	163	35,2	0,1	28,9	0,1	34,3		Segmento 4, Micropilote 3	13	163	28,9	34,3	31,6
	Segmento 5, Micropilote 3	13	160	35,2	0,1	28,9	0,1	33,8		Segmento 5, Micropilote 3	13	160	28,9	33,8	31,3
3	Segmento 6, Micropilote 3	21	159	35,2	0,1	47,4	0,1	33,5		Segmento 6, Micropilote 3	21	159	47,4	33,5	40,5
	Segmento 7, Micropilote 3	26	158	35,2	0,1	58,7	0,1	33,3		Segmento 7, Micropilote 3	26	158	58,7	33,3	46,0
	Segmento 8, Micropilote 3	22	156	35,2	0,1	50,3	0,1	32,9		Segmento 8, Micropilote 3	22	156	50,3	32,9	41,6
	Segmento 9, Micropilote 3	19	157	35,2	0,1	42,4	0,1	33,1		Segmento 9, Micropilote 3	19	157	42,4	33,1	37,8
	Segmento 10, Micropilote 3	21	157	35,2	0,1	46,5	0,1	33,1		Segmento 10, Micropilote 3	21	157	46,5	33,1	39,8
	Segmento 11, Micropilote 3	18	159	35,2	0,1	39,7	0,1	33,4		Segmento 11, Micropilote 3	18	159	39,7	33,4	36,6
	Segmento 12, Micropilote 3	26	262	35,2	0,1	58,2	0,1	55,2		Segmento 12, Micropilote 3	26	262	58,2	55,2	56,7
		3	156	41,3	0,0	6,6	0,1	38,6			3	156	6,6	38,6	22,6
		3	159	41,3	0,0	7,9	0,1	39,3			3	159	7,9	39,3	23,6
		4	157	41,3	0,0	10,1	0,1	38,8			4	157	10,1	38,8	24,4
		13	163	41,3	0,1	33,9	0,1	40,2			13	163	33,9	40,2	37,1
		13	160	41,3	0,1	33,9	0,1	39,6			13	160	33,9	39,6	36,8
5		21	159	41,3	0,1	55,6	0,1	39,3			21	159	55,6	39,3	47,5
		26	158	41,3	0,1	68,9	0,1	39,1			26	158	68,9	39,1	54,0
		22	156	41,3	0,1	59,1	0,1	38,6			22	156	59,1	38,6	48,9
		19	157	41,3	0,1	49,8	0,1	38,8			19	157	49,8	38,8	44,3
		21	157	41,3	0,1	54,6	0,1	38,8			21	157	54,6	38,8	46,7
		18	159	41,3	0,1	46,6	0,1	39,2			18	159	46,6	39,2	42,9
		26	262	41,3	0,1	68,3	0,1	64,8			26	262	68,3	64,8	66,5
		3	156	34,6	0,0	5,6	0,1	32,4			3	156	5,6	32,4	19,0
		3	159	34,6	0,0	6,7	0,1	32,9			3	159	6,7	32,9	19,8
		4	157	34,6	0,0	8,4	0,1	32,6			4	157	8,4	32,6	20,5
		13	163	34,6	0,1	28,4	0,1	33,8			13	163	28,4	33,8	31,1
		13	160	34,6	0,1	28,4	0,1	33,3			13	160	28,4	33,3	30,8
6		21	159	34,6	0,1	46,7	0,1	33,0			21	159	46,7	33,0	39,8
		26	158	34,6	0,1	57,8	0,1	32,8			26	158	57,8	32,8	45,3
		22	156	34,6	0,1	49,6	0,1	32,4			22	156	49,6	32,4	41,0
		19	157	34,6	0,1	41,8	0,1	32,6			19	157	41,8	32,6	37,2
		21	157	34,6	0,1	45,8	0,1	32,6			21	157	45,8	32,6	39,2
		18	159	34,6	0,1	39,1	0,1	32,9			18	159	39,1	32,9	36,0
		26	262	34,6	0,1	57,3	0,1	54,3			26	262	57,3	54,3	55,8

	Analysis Segment	Nspt, avg	Shear Wave Vel, Vs_avg [m/s]	Shear Strenght at Qu [kN/m2]	Nspt_i/ΣN spt	Ti (spt) [kN/m2]	Vs_i/ΣVs	Ti_(Vs) [kN/m2]	Ti_(Vs-Nspt) [kN/m2]	Analysis Segment	N _ Mean/m	Shear Wave Vel (VS)_Mean [m/s]	Ti_spt (kN/m2)	Ti_Vs (kN/m2)	Ti_Vs-Nspt (kN/m2)
	Segmento 1, Micropilote 3	3	156	35,2	0,0	5,6	0,1	32,9		Segmento 1, Micropilote 3	3	156	5,6	32,9	19,3
	Segmento 2, Micropilote 3	3	159	35,2	0,0	6,8	0,1	33,5		Segmento 2, Micropilote 3	3	159	6,8	33,5	20,1
	Segmento 3, Micropilote 3	4	157	35,2	0,0	8,6	0,1	33,1		Segmento 3, Micropilote 3	4	157	8,6	33,1	20,8
	Segmento 4, Micropilote 3	13	163	35,2	0,1	28,9	0,1	34,3		Segmento 4, Micropilote 3	13	163	28,9	34,3	31,6
	Segmento 5, Micropilote 3	13	160	35,2	0,1	28,9	0,1	33,8		Segmento 5, Micropilote 3	13	160	28,9	33,8	31,3
3	Segmento 6, Micropilote 3	21	159	35,2	0,1	47,4	0,1	33,5		Segmento 6, Micropilote 3	21	159	47,4	33,5	40,5
	Segmento 7, Micropilote 3	26	158	35,2	0,1	58,7	0,1	33,3		Segmento 7, Micropilote 3	26	158	58,7	33,3	46,0
	Segmento 8, Micropilote 3	22	156	35,2	0,1	50,3	0,1	32,9		Segmento 8, Micropilote 3	22	156	50,3	32,9	41,6
	Segmento 9, Micropilote 3	19	157	35,2	0,1	42,4	0,1	33,1		Segmento 9, Micropilote 3	19	157	42,4	33,1	37,8
	Segmento 10, Micropilote 3	21	157	35,2	0,1	46,5	0,1	33,1		Segmento 10, Micropilote 3	21	157	46,5	33,1	39,8
	Segmento 11, Micropilote 3	18	159	35,2	0,1	39,7	0,1	33,4		Segmento 11, Micropilote 3	18	159	39,7	33,4	36,6
	Segmento 12, Micropilote 3	26	262	35,2	0,1	58,2	0,1	55,2		Segmento 12, Micropilote 3	26	262	58,2	55,2	56,7
		3	156	58,1	0,0	9,3	0,1	54,3			3	156	9,3	54,3	31,8
		3	159	58,1	0,0	11,2	0,1	55,2			3	159	11,2	55,2	33,2
		4	157	58,1	0,0	14,2	0,1	54,6			4	157	14,2	54,6	34,4
		13	163	58,1	0,1	47,7	0,1	56,6			13	163	47,7	56,6	52,2
		13	160	58,1	0,1	47,7	0,1	55,8			13	160	47,7	55,8	51,7
7		21	159	58,1	0,1	78,2	0,1	55,3			21	159	78,2	55,3	66,8
		26	158	58,1	0,1	96,9	0,1	55,0			26	158	96,9	55,0	75,9
		22	156	58,1	0,1	83,1	0,1	54,4			22	156	83,1	54,4	68,7
		19	157	58,1	0,1	70,0	0,1	54,6			19	157	70,0	54,6	62,3
		21	157	58,1	0,1	76,8	0,1	54,6			21	157	76,8	54,6	65,7
		18	159	58,1	0,1	65,6	0,1	55,2			18	159	65,6	55,2	60,4
		26	262	58,1	0,1	96,1	0,1	91,1			26	262	96,1	91,1	93,6
		3	156	44,9	0,0	7,2	0,1	42,0			3	156	7,2	42,0	24,6
		3	159	44,9	0,0	8,7	0,1	42,8			3	159	8,7	42,8	25,7
		4	157	44,9	0,0	11,0	0,1	42,3			4	157	11,0	42,3	26,6
		13	163	44,9	0,1	36,9	0,1	43,8			13	163	36,9	43,8	40,4
		13	160	44,9	0,1	36,9	0,1	43,2			13	160	36,9	43,2	40,0
8		21	159	44,9	0,1	60,6	0,1	42,8			21	159	60,6	42,8	51,7
		26	158	44,9	0,1	75,0	0,1	42,5			26	158	75,0	42,5	58,8
		22	156	44,9	0,1	64,3	0,1	42,1			22	156	64,3	42,1	53,2
		19	157	44,9	0,1	54,2	0,1	42,3			19	157	54,2	42,3	48,3
		21	157	44,9	0,1	59,4	0,1	42,3			21	157	59,4	42,3	50,9
		18	159	44,9	0,1	50,8	0,1	42,7			18	159	50,8	42,7	46,7
		26	262	44,9	0,1	74,4	0,1	70,5			26	262	74,4	70,5	72,5

	Analysis Segment	Nspt, avg	Shear Wave Vel, Vs_avg [m/s]	Shear Strenght at Qu [kN/m2]	Nspt_i/ΣN spt	Ti (spt) [kN/m2]	Vs_i/ΣVs	Ti_(Vs) [kN/m2]	Ti_(Vs-Nspt) [kN/m2]	Analysis Segment	N _ Mean/m	Shear Wave Vel (VS)_Mean [m/s]	Ti_spt (kN/m2)	Ti_Vs (kN/m2)	Ti_Vs-Nspt (kN/m2)
3	Segmento 1, Micropilote 3	3	156	35,2	0,0	5,6	0,1	32,9		Segmento 1, Micropilote 3	3	156	5,6	32,9	19,3
	Segmento 2, Micropilote 3	3	159	35,2	0,0	6,8	0,1	33,5		Segmento 2, Micropilote 3	3	159	6,8	33,5	20,1
	Segmento 3, Micropilote 3	4	157	35,2	0,0	8,6	0,1	33,1		Segmento 3, Micropilote 3	4	157	8,6	33,1	20,8
	Segmento 4, Micropilote 3	13	163	35,2	0,1	28,9	0,1	34,3		Segmento 4, Micropilote 3	13	163	28,9	34,3	31,6
	Segmento 5, Micropilote 3	13	160	35,2	0,1	28,9	0,1	33,8		Segmento 5, Micropilote 3	13	160	28,9	33,8	31,3
	Segmento 6, Micropilote 3	21	159	35,2	0,1	47,4	0,1	33,5		Segmento 6, Micropilote 3	21	159	47,4	33,5	40,5
	Segmento 7, Micropilote 3	26	158	35,2	0,1	58,7	0,1	33,3		Segmento 7, Micropilote 3	26	158	58,7	33,3	46,0
	Segmento 8, Micropilote 3	22	156	35,2	0,1	50,3	0,1	32,9		Segmento 8, Micropilote 3	22	156	50,3	32,9	41,6
	Segmento 9, Micropilote 3	19	157	35,2	0,1	42,4	0,1	33,1		Segmento 9, Micropilote 3	19	157	42,4	33,1	37,8
	Segmento 10, Micropilote 3	21	157	35,2	0,1	46,5	0,1	33,1		Segmento 10, Micropilote 3	21	157	46,5	33,1	39,8
	Segmento 11, Micropilote 3	18	159	35,2	0,1	39,7	0,1	33,4		Segmento 11, Micropilote 3	18	159	39,7	33,4	36,6
	Segmento 12, Micropilote 3	26	262	35,2	0,1	58,2	0,1	55,2		Segmento 12, Micropilote 3	26	262	58,2	55,2	56,7
9		3	156	37,8	0,0	6,1	0,1	35,3			3	156	6,1	35,3	20,7
		3	159	37,8	0,0	7,3	0,1	35,9			3	159	7,3	35,9	21,6
		4	157	37,8	0,0	9,2	0,1	35,5			4	157	9,2	35,5	22,4
		13	163	37,8	0,1	31,0	0,1	36,8			13	163	31,0	36,8	33,9
		13	160	37,8	0,1	31,0	0,1	36,3			13	160	31,0	36,3	33,6
		21	159	37,8	0,1	50,9	0,1	36,0			21	159	50,9	36,0	43,4
		26	158	37,8	0,1	63,0	0,1	35,7			26	158	63,0	35,7	49,4
		22	156	37,8	0,1	54,0	0,1	35,4			22	156	54,0	35,4	44,7
		19	157	37,8	0,1	45,5	0,1	35,5			19	157	45,5	35,5	40,5
		21	157	37,8	0,1	49,9	0,1	35,5			21	157	49,9	35,5	42,7
		18	159	37,8	0,1	42,6	0,1	35,9			18	159	42,6	35,9	39,3
		26	262	37,8	0,1	62,5	0,1	59,3			26	262	62,5	59,3	60,9
10		3	156	41,6	0,0	6,7	0,1	38,9			3	156	6,7	38,9	22,8
		3	159	41,6	0,0	8,0	0,1	39,6			3	159	8,0	39,6	23,8
		4	157	41,6	0,0	10,1	0,1	39,1			4	157	10,1	39,1	24,6
		13	163	41,6	0,1	34,2	0,1	40,6			13	163	34,2	40,6	37,4
		13	160	41,6	0,1	34,2	0,1	40,0			13	160	34,2	40,0	37,1
		21	159	41,6	0,1	56,1	0,1	39,6			21	159	56,1	39,6	47,9
		26	158	41,6	0,1	69,4	0,1	39,4			26	158	69,4	39,4	54,4
		22	156	41,6	0,1	59,5	0,1	39,0			22	156	59,5	39,0	49,3
		19	157	41,6	0,1	50,2	0,1	39,1			19	157	50,2	39,1	44,7
		21	157	41,6	0,1	55,0	0,1	39,1			21	157	55,0	39,1	47,1
		18	159	41,6	0,1	47,0	0,1	39,5			18	159	47,0	39,5	43,3
		26	262	41,6	0,1	68,9	0,1	65,3			26	262	68,9	65,3	67,1

	Analysis Segment	Nspt, avg	Shear Wave Vel, Vs_avg [m/s]	Shear Strenght at Qu [kN/m2]	Nspt_i/ΣN spt	Ti (spt) [kN/m2]	Vs_i/ΣVs	Ti_(Vs) [kN/m2]	Ti_(Vs-Nspt) [kN/m2]	Analysis Segment	N _ Mean/m	Shear Wave Vel (VS)_Mean [m/s]	Ti_spt (kN/m2)	Ti_Vs (kN/m2)	Ti_Vs-Nspt (kN/m2)
3	Segmento 1, Micropilote 3	3	156	35,2	0,0	5,6	0,1	32,9		Segmento 1, Micropilote 3	3	156	5,6	32,9	19,3
	Segmento 2, Micropilote 3	3	159	35,2	0,0	6,8	0,1	33,5		Segmento 2, Micropilote 3	3	159	6,8	33,5	20,1
	Segmento 3, Micropilote 3	4	157	35,2	0,0	8,6	0,1	33,1		Segmento 3, Micropilote 3	4	157	8,6	33,1	20,8
	Segmento 4, Micropilote 3	13	163	35,2	0,1	28,9	0,1	34,3		Segmento 4, Micropilote 3	13	163	28,9	34,3	31,6
	Segmento 5, Micropilote 3	13	160	35,2	0,1	28,9	0,1	33,8		Segmento 5, Micropilote 3	13	160	28,9	33,8	31,3
	Segmento 6, Micropilote 3	21	159	35,2	0,1	47,4	0,1	33,5		Segmento 6, Micropilote 3	21	159	47,4	33,5	40,5
	Segmento 7, Micropilote 3	26	158	35,2	0,1	58,7	0,1	33,3		Segmento 7, Micropilote 3	26	158	58,7	33,3	46,0
	Segmento 8, Micropilote 3	22	156	35,2	0,1	50,3	0,1	32,9		Segmento 8, Micropilote 3	22	156	50,3	32,9	41,6
	Segmento 9, Micropilote 3	19	157	35,2	0,1	42,4	0,1	33,1		Segmento 9, Micropilote 3	19	157	42,4	33,1	37,8
	Segmento 10, Micropilote 3	21	157	35,2	0,1	46,5	0,1	33,1		Segmento 10, Micropilote 3	21	157	46,5	33,1	39,8
	Segmento 11, Micropilote 3	18	159	35,2	0,1	39,7	0,1	33,4		Segmento 11, Micropilote 3	18	159	39,7	33,4	36,6
	Segmento 12, Micropilote 3	26	262	35,2	0,1	58,2	0,1	55,2		Segmento 12, Micropilote 3	26	262	58,2	55,2	56,7
11		3	156	52,8	0,0	8,5	0,1	49,4			3	156	8,5	49,4	28,9
		3	159	52,8	0,0	10,2	0,1	50,2			3	159	10,2	50,2	30,2
		4	157	52,8	0,0	12,9	0,1	49,6			4	157	12,9	49,6	31,3
		13	163	52,8	0,1	43,4	0,1	51,5			13	163	43,4	51,5	47,4
		13	160	52,8	0,1	43,4	0,1	50,7			13	160	43,4	50,7	47,0
		21	159	52,8	0,1	71,1	0,1	50,3			21	159	71,1	50,3	60,7
		26	158	52,8	0,1	88,1	0,1	50,0			26	158	88,1	50,0	69,0
		22	156	52,8	0,1	75,5	0,1	49,4			22	156	75,5	49,4	62,5
		19	157	52,8	0,1	63,7	0,1	49,7			19	157	63,7	49,7	56,7
		21	157	52,8	0,1	69,8	0,1	49,7			21	157	69,8	49,7	59,7
		18	159	52,8	0,1	59,6	0,1	50,2			18	159	59,6	50,2	54,9
		26	262	52,8	0,1	87,4	0,1	82,8			26	262	87,4	82,8	85,1
12		3	156	47,9	0,0	7,7	0,1	44,8			3	156	7,7	44,8	26,2
		3	159	47,9	0,0	9,2	0,1	45,6			3	159	9,2	45,6	27,4
		4	157	47,9	0,0	11,7	0,1	45,0			4	157	11,7	45,0	28,4
		13	163	47,9	0,1	39,3	0,1	46,7			13	163	39,3	46,7	43,0
		13	160	47,9	0,1	39,3	0,1	46,0			13	160	39,3	46,0	42,7
		21	159	47,9	0,1	64,5	0,1	45,6			21	159	64,5	45,6	55,1
		26	158	47,9	0,1	79,9	0,1	45,3			26	158	79,9	45,3	62,6
		22	156	47,9	0,1	68,5	0,1	44,9			22	156	68,5	44,9	56,7
		19	157	47,9	0,1	57,8	0,1	45,1			19	157	57,8	45,1	51,4
		21	157	47,9	0,1	63,3	0,1	45,1			21	157	63,3	45,1	54,2
		18	159	47,9	0,1	54,1	0,1	45,5			18	159	54,1	45,5	49,8
		26	262	47,9	0,1	79,3	0,1	75,2			26	262	79,3	75,2	77,2

	Analysis Segment	Nspt, avg	Shear Wave Vel, Vs_avg [m/s]	Shear Strenght at Qu [kN/m2]	Nspt_i/ΣN spt	Ti (spt) [kN/m2]	Vs_i/ΣVs	Ti_(Vs) [kN/m2]	Ti_(Vs-Nspt) [kN/m2]	Analysis Segment	N _ Mean/m	Shear Wave Vel (VS)_Mean [m/s]	Ti_spt (kN/m2)	Ti_Vs (kN/m2)	Ti_Vs-Nspt (kN/m2)
3	Segmento 1, Micropilote 3	3	156	35,2	0,0	5,6	0,1	32,9		Segmento 1, Micropilote 3	3	156	5,6	32,9	19,3
	Segmento 2, Micropilote 3	3	159	35,2	0,0	6,8	0,1	33,5		Segmento 2, Micropilote 3	3	159	6,8	33,5	20,1
	Segmento 3, Micropilote 3	4	157	35,2	0,0	8,6	0,1	33,1		Segmento 3, Micropilote 3	4	157	8,6	33,1	20,8
	Segmento 4, Micropilote 3	13	163	35,2	0,1	28,9	0,1	34,3		Segmento 4, Micropilote 3	13	163	28,9	34,3	31,6
	Segmento 5, Micropilote 3	13	160	35,2	0,1	28,9	0,1	33,8		Segmento 5, Micropilote 3	13	160	28,9	33,8	31,3
	Segmento 6, Micropilote 3	21	159	35,2	0,1	47,4	0,1	33,5		Segmento 6, Micropilote 3	21	159	47,4	33,5	40,5
	Segmento 7, Micropilote 3	26	158	35,2	0,1	58,7	0,1	33,3		Segmento 7, Micropilote 3	26	158	58,7	33,3	46,0
	Segmento 8, Micropilote 3	22	156	35,2	0,1	50,3	0,1	32,9		Segmento 8, Micropilote 3	22	156	50,3	32,9	41,6
	Segmento 9, Micropilote 3	19	157	35,2	0,1	42,4	0,1	33,1		Segmento 9, Micropilote 3	19	157	42,4	33,1	37,8
	Segmento 10, Micropilote 3	21	157	35,2	0,1	46,5	0,1	33,1		Segmento 10, Micropilote 3	21	157	46,5	33,1	39,8
	Segmento 11, Micropilote 3	18	159	35,2	0,1	39,7	0,1	33,4		Segmento 11, Micropilote 3	18	159	39,7	33,4	36,6
	Segmento 12, Micropilote 3	26	262	35,2	0,1	58,2	0,1	55,2		Segmento 12, Micropilote 3	26	262	58,2	55,2	56,7
13		3	156	41,1	0,0	6,6	0,1	38,5			3	156	6,6	38,5	22,5
		3	159	41,1	0,0	7,9	0,1	39,1			3	159	7,9	39,1	23,5
		4	157	41,1	0,0	10,0	0,1	38,7			4	157	10,0	38,7	24,4
		13	163	41,1	0,1	33,8	0,1	40,1			13	163	33,8	40,1	37,0
		13	160	41,1	0,1	33,8	0,1	39,5			13	160	33,8	39,5	36,6
		21	159	41,1	0,1	55,4	0,1	39,2			21	159	55,4	39,2	47,3
		26	158	41,1	0,1	68,6	0,1	38,9			26	158	68,6	38,9	53,8
		22	156	41,1	0,1	58,9	0,1	38,5			22	156	58,9	38,5	48,7
		19	157	41,1	0,1	49,6	0,1	38,7			19	157	49,6	38,7	44,2
		21	157	41,1	0,1	54,4	0,1	38,7			21	157	54,4	38,7	46,5
		18	159	41,1	0,1	46,5	0,1	39,1			18	159	46,5	39,1	42,8
		26	262	41,1	0,1	68,1	0,1	64,6			26	262	68,1	64,6	66,3
14		3	156	48,5	0,0	7,8	0,1	45,4			3	156	7,8	45,4	26,6
		3	159	48,5	0,0	9,3	0,1	46,1			3	159	9,3	46,1	27,7
		4	157	48,5	0,0	11,8	0,1	45,6			4	157	11,8	45,6	28,7
		13	163	48,5	0,1	39,8	0,1	47,3			13	163	39,8	47,3	43,6
		13	160	48,5	0,1	39,8	0,1	46,6			13	160	39,8	46,6	43,2
		21	159	48,5	0,1	65,3	0,1	46,2			21	159	65,3	46,2	55,8
		26	158	48,5	0,1	80,9	0,1	45,9			26	158	80,9	45,9	63,4
		22	156	48,5	0,1	69,4	0,1	45,4			22	156	69,4	45,4	57,4
		19	157	48,5	0,1	58,5	0,1	45,6			19	157	58,5	45,6	52,1
		21	157	48,5	0,1	64,1	0,1	45,6			21	157	64,1	45,6	54,9
		18	159	48,5	0,1	54,8	0,1	46,1			18	159	54,8	46,1	50,4
		26	262	48,5	0,1	80,3	0,1	76,1			26	262	80,3	76,1	78,2

	Analysis Segment	Nspt, avg	Shear Wave Vel, Vs_avg [m/s]	Shear Strenght at Qu [kN/m2]	Nspt_i/ΣN spt	Ti (spt) [kN/m2]	Vs_i/ΣVs	Ti_(Vs) [kN/m2]	Ti_(Vs-Nspt) [kN/m2]	Analysis Segment	N _ Mean/m	Shear Wave Vel (VS)_Mean [m/s]	Ti_spt (kN/m2)	Ti_Vs (kN/m2)	Ti_Vs-Nspt (kN/m2)
3	Segmento 1, Micropilote 3	3	156	35,2	0,0	5,6	0,1	32,9		Segmento 1, Micropilote 3	3	156	5,6	32,9	19,3
	Segmento 2, Micropilote 3	3	159	35,2	0,0	6,8	0,1	33,5		Segmento 2, Micropilote 3	3	159	6,8	33,5	20,1
	Segmento 3, Micropilote 3	4	157	35,2	0,0	8,6	0,1	33,1		Segmento 3, Micropilote 3	4	157	8,6	33,1	20,8
	Segmento 4, Micropilote 3	13	163	35,2	0,1	28,9	0,1	34,3		Segmento 4, Micropilote 3	13	163	28,9	34,3	31,6
	Segmento 5, Micropilote 3	13	160	35,2	0,1	28,9	0,1	33,8		Segmento 5, Micropilote 3	13	160	28,9	33,8	31,3
	Segmento 6, Micropilote 3	21	159	35,2	0,1	47,4	0,1	33,5		Segmento 6, Micropilote 3	21	159	47,4	33,5	40,5
	Segmento 7, Micropilote 3	26	158	35,2	0,1	58,7	0,1	33,3		Segmento 7, Micropilote 3	26	158	58,7	33,3	46,0
	Segmento 8, Micropilote 3	22	156	35,2	0,1	50,3	0,1	32,9		Segmento 8, Micropilote 3	22	156	50,3	32,9	41,6
	Segmento 9, Micropilote 3	19	157	35,2	0,1	42,4	0,1	33,1		Segmento 9, Micropilote 3	19	157	42,4	33,1	37,8
	Segmento 10, Micropilote 3	21	157	35,2	0,1	46,5	0,1	33,1		Segmento 10, Micropilote 3	21	157	46,5	33,1	39,8
	Segmento 11, Micropilote 3	18	159	35,2	0,1	39,7	0,1	33,4		Segmento 11, Micropilote 3	18	159	39,7	33,4	36,6
	Segmento 12, Micropilote 3	26	262	35,2	0,1	58,2	0,1	55,2		Segmento 12, Micropilote 3	26	262	58,2	55,2	56,7
15		3	156	53,5	0,0	8,6	0,1	50,0			3	156	8,6	50,0	29,3
		3	159	53,5	0,0	10,3	0,1	50,9			3	159	10,3	50,9	30,6
		4	157	53,5	0,0	13,0	0,1	50,3			4	157	13,0	50,3	31,7
		13	163	53,5	0,1	43,9	0,1	52,1			13	163	43,9	52,1	48,0
		13	160	53,5	0,1	43,9	0,1	51,3			13	160	43,9	51,3	47,6
		21	159	53,5	0,1	72,0	0,1	50,9			21	159	72,0	50,9	61,5
		26	158	53,5	0,1	89,2	0,1	50,6			26	158	89,2	50,6	69,9
		22	156	53,5	0,1	76,5	0,1	50,1			22	156	76,5	50,1	63,3
		19	157	53,5	0,1	64,5	0,1	50,3			19	157	64,5	50,3	57,4
		21	157	53,5	0,1	70,7	0,1	50,3			21	157	70,7	50,3	60,5
		18	159	53,5	0,1	60,4	0,1	50,8			18	159	60,4	50,8	55,6
		26	262	53,5	0,1	88,5	0,1	83,9			26	262	88,5	83,9	86,2
16		3	156	38,4	0,0	6,2	0,1	35,9			3	156	6,2	35,9	21,0
		3	159	38,4	0,0	7,4	0,1	36,5			3	159	7,4	36,5	21,9
		4	157	38,4	0,0	9,4	0,1	36,1			4	157	9,4	36,1	22,7
		13	163	38,4	0,1	31,5	0,1	37,4			13	163	31,5	37,4	34,5
		13	160	38,4	0,1	31,5	0,1	36,8			13	160	31,5	36,8	34,2
		21	159	38,4	0,1	51,7	0,1	36,5			21	159	51,7	36,5	44,1
		26	158	38,4	0,1	64,0	0,1	36,3			26	158	64,0	36,3	50,2
		22	156	38,4	0,1	54,9	0,1	35,9			22	156	54,9	35,9	45,4
		19	157	38,4	0,1	46,3	0,1	36,1			19	157	46,3	36,1	41,2
		21	157	38,4	0,1	50,7	0,1	36,1			21	157	50,7	36,1	43,4
		18	159	38,4	0,1	43,3	0,1	36,5			18	159	43,3	36,5	39,9
		26	262	38,4	0,1	63,5	0,1	60,2			26	262	63,5	60,2	61,9

	Analysis Segment	Nspt, avg	Shear Wave Vel, Vs_avg [m/s]	Shear Strenght at Qu [kN/m2]	Nspt_i/ΣN spt	Ti (spt) [kN/m2]	Vs_i/ΣVs	Ti_(Vs) [kN/m2]	Ti_(Vs-Nspt) [kN/m2]	Analysis Segment	N _ Mean/m	Shear Wave Vel (VS)_Mean [m/s]	Ti_spt (kN/m2)	Ti_Vs (kN/m2)	Ti_Vs-Nspt (kN/m2)
3	Segmento 1, Micropilote 3	3	156	35,2	0,0	5,6	0,1	32,9		Segmento 1, Micropilote 3	3	156	5,6	32,9	19,3
	Segmento 2, Micropilote 3	3	159	35,2	0,0	6,8	0,1	33,5		Segmento 2, Micropilote 3	3	159	6,8	33,5	20,1
	Segmento 3, Micropilote 3	4	157	35,2	0,0	8,6	0,1	33,1		Segmento 3, Micropilote 3	4	157	8,6	33,1	20,8
	Segmento 4, Micropilote 3	13	163	35,2	0,1	28,9	0,1	34,3		Segmento 4, Micropilote 3	13	163	28,9	34,3	31,6
	Segmento 5, Micropilote 3	13	160	35,2	0,1	28,9	0,1	33,8		Segmento 5, Micropilote 3	13	160	28,9	33,8	31,3
	Segmento 6, Micropilote 3	21	159	35,2	0,1	47,4	0,1	33,5		Segmento 6, Micropilote 3	21	159	47,4	33,5	40,5
	Segmento 7, Micropilote 3	26	158	35,2	0,1	58,7	0,1	33,3		Segmento 7, Micropilote 3	26	158	58,7	33,3	46,0
	Segmento 8, Micropilote 3	22	156	35,2	0,1	50,3	0,1	32,9		Segmento 8, Micropilote 3	22	156	50,3	32,9	41,6
	Segmento 9, Micropilote 3	19	157	35,2	0,1	42,4	0,1	33,1		Segmento 9, Micropilote 3	19	157	42,4	33,1	37,8
	Segmento 10, Micropilote 3	21	157	35,2	0,1	46,5	0,1	33,1		Segmento 10, Micropilote 3	21	157	46,5	33,1	39,8
	Segmento 11, Micropilote 3	18	159	35,2	0,1	39,7	0,1	33,4		Segmento 11, Micropilote 3	18	159	39,7	33,4	36,6
	Segmento 12, Micropilote 3	26	262	35,2	0,1	58,2	0,1	55,2		Segmento 12, Micropilote 3	26	262	58,2	55,2	56,7
17		3	156	38,1	0,0	6,1	0,1	35,6			3	156	6,1	35,6	20,9
		3	159	38,1	0,0	7,3	0,1	36,2			3	159	7,3	36,2	21,8
		4	157	38,1	0,0	9,3	0,1	35,8			4	157	9,3	35,8	22,5
		13	163	38,1	0,1	31,3	0,1	37,1			13	163	31,3	37,1	34,2
		13	160	38,1	0,1	31,3	0,1	36,6			13	160	31,3	36,6	33,9
		21	159	38,1	0,1	51,3	0,1	36,3			21	159	51,3	36,3	43,8
		26	158	38,1	0,1	63,5	0,1	36,0			26	158	63,5	36,0	49,8
		22	156	38,1	0,1	54,5	0,1	35,7			22	156	54,5	35,7	45,1
		19	157	38,1	0,1	45,9	0,1	35,8			19	157	45,9	35,8	40,9
		21	157	38,1	0,1	50,3	0,1	35,8			21	157	50,3	35,8	43,1
		18	159	38,1	0,1	43,0	0,1	36,2			18	159	43,0	36,2	39,6
		26	262	38,1	0,1	63,0	0,1	59,8			26	262	63,0	59,8	61,4
18		3	156	48,1	0,0	7,7	0,1	45,0			3	156	7,7	45,0	26,3
		3	159	48,1	0,0	9,3	0,1	45,7			3	159	9,3	45,7	27,5
		4	157	48,1	0,0	11,7	0,1	45,2			4	157	11,7	45,2	28,5
		13	163	48,1	0,1	39,5	0,1	46,9			13	163	39,5	46,9	43,2
		13	160	48,1	0,1	39,5	0,1	46,2			13	160	39,5	46,2	42,8
		21	159	48,1	0,1	64,8	0,1	45,8			21	159	64,8	45,8	55,3
		26	158	48,1	0,1	80,2	0,1	45,5			26	158	80,2	45,5	62,9
		22	156	48,1	0,1	68,8	0,1	45,0			22	156	68,8	45,0	56,9
		19	157	48,1	0,1	58,0	0,1	45,2			19	157	58,0	45,2	51,6
		21	157	48,1	0,1	63,6	0,1	45,2			21	157	63,6	45,2	54,4
		18	159	48,1	0,1	54,3	0,1	45,7			18	159	54,3	45,7	50,0
		26	262	48,1	0,1	79,6	0,1	75,5			26	262	79,6	75,5	77,5

	Analysis Segment	Nspt, avg	Shear Wave Vel, Vs_avg [m/s]	Shear Strenght at Qu [kN/m2]	Nspt_i/ΣN spt	Ti (spt) [kN/m2]	Vs_i/ΣVs	Ti_(Vs) [kN/m2]	Ti_(Vs-Nspt) [kN/m2]	Analysis Segment	N _ Mean/m	Shear Wave Vel (VS)_Mean [m/s]	Ti_spt (kN/m2)	Ti_Vs (kN/m2)	Ti_Vs-Nspt (kN/m2)
3	Segmento 1, Micropilote 3	3	156	35,2	0,0	5,6	0,1	32,9		Segmento 1, Micropilote 3	3	156	5,6	32,9	19,3
	Segmento 2, Micropilote 3	3	159	35,2	0,0	6,8	0,1	33,5		Segmento 2, Micropilote 3	3	159	6,8	33,5	20,1
	Segmento 3, Micropilote 3	4	157	35,2	0,0	8,6	0,1	33,1		Segmento 3, Micropilote 3	4	157	8,6	33,1	20,8
	Segmento 4, Micropilote 3	13	163	35,2	0,1	28,9	0,1	34,3		Segmento 4, Micropilote 3	13	163	28,9	34,3	31,6
	Segmento 5, Micropilote 3	13	160	35,2	0,1	28,9	0,1	33,8		Segmento 5, Micropilote 3	13	160	28,9	33,8	31,3
	Segmento 6, Micropilote 3	21	159	35,2	0,1	47,4	0,1	33,5		Segmento 6, Micropilote 3	21	159	47,4	33,5	40,5
	Segmento 7, Micropilote 3	26	158	35,2	0,1	58,7	0,1	33,3		Segmento 7, Micropilote 3	26	158	58,7	33,3	46,0
	Segmento 8, Micropilote 3	22	156	35,2	0,1	50,3	0,1	32,9		Segmento 8, Micropilote 3	22	156	50,3	32,9	41,6
	Segmento 9, Micropilote 3	19	157	35,2	0,1	42,4	0,1	33,1		Segmento 9, Micropilote 3	19	157	42,4	33,1	37,8
	Segmento 10, Micropilote 3	21	157	35,2	0,1	46,5	0,1	33,1		Segmento 10, Micropilote 3	21	157	46,5	33,1	39,8
	Segmento 11, Micropilote 3	18	159	35,2	0,1	39,7	0,1	33,4		Segmento 11, Micropilote 3	18	159	39,7	33,4	36,6
	Segmento 12, Micropilote 3	26	262	35,2	0,1	58,2	0,1	55,2		Segmento 12, Micropilote 3	26	262	58,2	55,2	56,7
19		3	156	27,1	0,0	4,3	0,1	25,3			3	156	4,3	25,3	14,8
		3	159	27,1	0,0	5,2	0,1	25,8			3	159	5,2	25,8	15,5
		4	157	27,1	0,0	6,6	0,1	25,5			4	157	6,6	25,5	16,0
		13	163	27,1	0,1	22,2	0,1	26,4			13	163	22,2	26,4	24,3
		13	160	27,1	0,1	22,2	0,1	26,0			13	160	22,2	26,0	24,1
		21	159	27,1	0,1	36,5	0,1	25,8			21	159	36,5	25,8	31,1
		26	158	27,1	0,1	45,2	0,1	25,6			26	158	45,2	25,6	35,4
		22	156	27,1	0,1	38,7	0,1	25,4			22	156	38,7	25,4	32,0
		19	157	27,1	0,1	32,7	0,1	25,5			19	157	32,7	25,5	29,1
		21	157	27,1	0,1	35,8	0,1	25,5			21	157	35,8	25,5	30,6
		18	159	27,1	0,1	30,6	0,1	25,7			18	159	30,6	25,7	28,2
		26	262	27,1	0,1	44,8	0,1	42,5			26	262	44,8	42,5	43,7
20		3	156	83,2	0,0	13,3	0,1	77,8			3	156	13,3	77,8	45,6
		3	159	83,2	0,0	16,0	0,1	79,1			3	159	16,0	79,1	47,6
		4	157	83,2	0,0	20,3	0,1	78,2			4	157	20,3	78,2	49,2
		13	163	83,2	0,1	68,3	0,1	81,1			13	163	68,3	81,1	74,7
		13	160	83,2	0,1	68,3	0,1	79,9			13	160	68,3	79,9	74,1
		21	159	83,2	0,1	112,1	0,1	79,2			21	159	112,1	79,2	95,6
		26	158	83,2	0,1	138,7	0,1	78,7			26	158	138,7	78,7	108,7
		22	156	83,2	0,1	119,0	0,1	77,9			22	156	119,0	77,9	98,4
		19	157	83,2	0,1	100,3	0,1	78,2			19	157	100,3	78,2	89,3
		21	157	83,2	0,1	109,9	0,1	78,2			21	157	109,9	78,2	94,1
		18	159	83,2	0,1	93,9	0,1	79,0			18	159	93,9	79,0	86,5
		26	262	83,2	0,1	137,7	0,1	130,5			26	262	137,7	130,5	134,1

	Analysis Segment	Nspt, avg	Shear Wave Vel, Vs_avg [m/s]	Shear Strenght at Qu [kN/m2]	Nspt_i/ΣNspt	Ti (spt) [kN/m2]	Vs_i/ΣVs	Ti_(Vs) [kN/m2]	Ti_(Vs-Nspt) [kN/m2]	Analysis Segment	N _ Mean/m	Shear Wave Vel (VS)_Mean [m/s]	Ti_spt (kN/m2)	Ti_Vs (kN/m2)	Ti_Vs-Nspt (kN/m2)
3	Segmento 1, Micropilote 3	3	156	35,2	0,0	5,6	0,1	32,9		Segmento 1, Micropilote 3	3	156	5,6	32,9	19,3
	Segmento 2, Micropilote 3	3	159	35,2	0,0	6,8	0,1	33,5		Segmento 2, Micropilote 3	3	159	6,8	33,5	20,1
	Segmento 3, Micropilote 3	4	157	35,2	0,0	8,6	0,1	33,1		Segmento 3, Micropilote 3	4	157	8,6	33,1	20,8
	Segmento 4, Micropilote 3	13	163	35,2	0,1	28,9	0,1	34,3		Segmento 4, Micropilote 3	13	163	28,9	34,3	31,6
	Segmento 5, Micropilote 3	13	160	35,2	0,1	28,9	0,1	33,8		Segmento 5, Micropilote 3	13	160	28,9	33,8	31,3
	Segmento 6, Micropilote 3	21	159	35,2	0,1	47,4	0,1	33,5		Segmento 6, Micropilote 3	21	159	47,4	33,5	40,5
	Segmento 7, Micropilote 3	26	158	35,2	0,1	58,7	0,1	33,3		Segmento 7, Micropilote 3	26	158	58,7	33,3	46,0
	Segmento 8, Micropilote 3	22	156	35,2	0,1	50,3	0,1	32,9		Segmento 8, Micropilote 3	22	156	50,3	32,9	41,6
	Segmento 9, Micropilote 3	19	157	35,2	0,1	42,4	0,1	33,1		Segmento 9, Micropilote 3	19	157	42,4	33,1	37,8
	Segmento 10, Micropilote 3	21	157	35,2	0,1	46,5	0,1	33,1		Segmento 10, Micropilote 3	21	157	46,5	33,1	39,8
	Segmento 11, Micropilote 3	18	159	35,2	0,1	39,7	0,1	33,4		Segmento 11, Micropilote 3	18	159	39,7	33,4	36,6
	Segmento 12, Micropilote 3	26	262	35,2	0,1	58,2	0,1	55,2		Segmento 12, Micropilote 3	26	262	58,2	55,2	56,7
36		3	156	42,3	0,0	6,8	0,1	39,5			3	156	6,8	39,5	23,2
		3	159	42,3	0,0	8,1	0,1	40,2			3	159	8,1	40,2	24,2
		4	157	42,3	0,0	10,3	0,1	39,8			4	157	10,3	39,8	25,0
		13	163	42,3	0,1	34,7	0,1	41,2			13	163	34,7	41,2	38,0
		13	160	42,3	0,1	34,7	0,1	40,6			13	160	34,7	40,6	37,7
		21	159	42,3	0,1	57,0	0,1	40,3			21	159	57,0	40,3	48,6
		26	158	42,3	0,1	70,5	0,1	40,0			26	158	70,5	40,0	55,3
		22	156	42,3	0,1	60,5	0,1	39,6			22	156	60,5	39,6	50,0
		19	157	42,3	0,1	51,0	0,1	39,8			19	157	51,0	39,8	45,4
		21	157	42,3	0,1	55,9	0,1	39,8			21	157	55,9	39,8	47,8
		18	159	42,3	0,1	47,7	0,1	40,2			18	159	47,7	40,2	44,0
		26	262	42,3	0,1	70,0	0,1	66,4			26	262	70,0	66,4	68,2
37		3	156	42,3	0,0	6,8	0,1	39,5			3	156	6,8	39,5	23,2
		3	159	42,3	0,0	8,1	0,1	40,2			3	159	8,1	40,2	24,2
		4	157	42,3	0,0	10,3	0,1	39,8			4	157	10,3	39,8	25,0
		13	163	42,3	0,1	34,7	0,1	41,2			13	163	34,7	41,2	38,0
		13	160	42,3	0,1	34,7	0,1	40,6			13	160	34,7	40,6	37,7
		21	159	42,3	0,1	57,0	0,1	40,3			21	159	57,0	40,3	48,6
		26	158	42,3	0,1	70,5	0,1	40,0			26	158	70,5	40,0	55,3
		22	156	42,3	0,1	60,5	0,1	39,6			22	156	60,5	39,6	50,0
		19	157	42,3	0,1	51,0	0,1	39,8			19	157	51,0	39,8	45,4
		21	157	42,3	0,1	55,9	0,1	39,8			21	157	55,9	39,8	47,8
		18	159	42,3	0,1	47,7	0,1	40,2			18	159	47,7	40,2	44,0
		26	262	42,3	0,1	70,0	0,1	66,4			26	262	70,0	66,4	68,2

	Analysis Segment	Nspt, avg	Shear Wave Vel, Vs_avg [m/s]	Shear Strenght at Qu [kN/m2]	Nspt_i/ΣNspt	Ti (spt) [kN/m2]	Vs_i/ΣVs	Ti_(Vs) [kN/m2]	Ti_(Vs-Nspt) [kN/m2]	Analysis Segment	N _ Mean/m	Shear Wave Vel (VS)_Mean [m/s]	Ti_spt (kN/m2)	Ti_Vs (kN/m2)	Ti_Vs-Nspt (kN/m2)
3	Segmento 1, Micropilote 3	3	156	35,2	0,0	5,6	0,1	32,9		Segmento 1, Micropilote 3	3	156	5,6	32,9	19,3
	Segmento 2, Micropilote 3	3	159	35,2	0,0	6,8	0,1	33,5		Segmento 2, Micropilote 3	3	159	6,8	33,5	20,1
	Segmento 3, Micropilote 3	4	157	35,2	0,0	8,6	0,1	33,1		Segmento 3, Micropilote 3	4	157	8,6	33,1	20,8
	Segmento 4, Micropilote 3	13	163	35,2	0,1	28,9	0,1	34,3		Segmento 4, Micropilote 3	13	163	28,9	34,3	31,6
	Segmento 5, Micropilote 3	13	160	35,2	0,1	28,9	0,1	33,8		Segmento 5, Micropilote 3	13	160	28,9	33,8	31,3
	Segmento 6, Micropilote 3	21	159	35,2	0,1	47,4	0,1	33,5		Segmento 6, Micropilote 3	21	159	47,4	33,5	40,5
	Segmento 7, Micropilote 3	26	158	35,2	0,1	58,7	0,1	33,3		Segmento 7, Micropilote 3	26	158	58,7	33,3	46,0
	Segmento 8, Micropilote 3	22	156	35,2	0,1	50,3	0,1	32,9		Segmento 8, Micropilote 3	22	156	50,3	32,9	41,6
	Segmento 9, Micropilote 3	19	157	35,2	0,1	42,4	0,1	33,1		Segmento 9, Micropilote 3	19	157	42,4	33,1	37,8
	Segmento 10, Micropilote 3	21	157	35,2	0,1	46,5	0,1	33,1		Segmento 10, Micropilote 3	21	157	46,5	33,1	39,8
	Segmento 11, Micropilote 3	18	159	35,2	0,1	39,7	0,1	33,4		Segmento 11, Micropilote 3	18	159	39,7	33,4	36,6
	Segmento 12, Micropilote 3	26	262	35,2	0,1	58,2	0,1	55,2		Segmento 12, Micropilote 3	26	262	58,2	55,2	56,7
38		3	156	42,3	0,0	6,8	0,1	39,5			3	156	6,8	39,5	23,2
		3	159	42,3	0,0	8,1	0,1	40,2			3	159	8,1	40,2	24,2
		4	157	42,3	0,0	10,3	0,1	39,8			4	157	10,3	39,8	25,0
		13	163	42,3	0,1	34,7	0,1	41,2			13	163	34,7	41,2	38,0
		13	160	42,3	0,1	34,7	0,1	40,6			13	160	34,7	40,6	37,7
		21	159	42,3	0,1	57,0	0,1	40,3			21	159	57,0	40,3	48,6
		26	158	42,3	0,1	70,5	0,1	40,0			26	158	70,5	40,0	55,3
		22	156	42,3	0,1	60,5	0,1	39,6			22	156	60,5	39,6	50,0
		19	157	42,3	0,1	51,0	0,1	39,8			19	157	51,0	39,8	45,4
		21	157	42,3	0,1	55,9	0,1	39,8			21	157	55,9	39,8	47,8
		18	159	42,3	0,1	47,7	0,1	40,2			18	159	47,7	40,2	44,0
		26	262	42,3	0,1	70,0	0,1	66,4			26	262	70,0	66,4	68,2
39		3	156	42,3	0,0	6,8	0,1	39,5			3	156	6,8	39,5	23,2
		3	159	42,3	0,0	8,1	0,1	40,2			3	159	8,1	40,2	24,2
		4	157	42,3	0,0	10,3	0,1	39,8			4	157	10,3	39,8	25,0
		13	163	42,3	0,1	34,7	0,1	41,2			13	163	34,7	41,2	38,0
		13	160	42,3	0,1	34,7	0,1	40,6			13	160	34,7	40,6	37,7
		21	159	42,3	0,1	57,0	0,1	40,3			21	159	57,0	40,3	48,6
		26	158	42,3	0,1	70,5	0,1	40,0			26	158	70,5	40,0	55,3
		22	156	42,3	0,1	60,5	0,1	39,6			22	156	60,5	39,6	50,0
		19	157	42,3	0,1	51,0	0,1	39,8			19	157	51,0	39,8	45,4
		21	157	42,3	0,1	55,9	0,1	39,8			21	157	55,9	39,8	47,8
		18	159	42,3	0,1	47,7	0,1	40,2			18	159	47,7	40,2	44,0
		26	262	42,3	0,1	70,0	0,1	66,4			26	262	70,0	66,4	68,2
40	Segmento 1, Micropilote 40	3	156	42,3	0,0	6,8	0,1	39,5	23,2	Segmento 1, Micropilote 40	3	156	6,8	39,5	23,2
	Segmento 2, Micropilote 40	3	159	42,3	0,0	8,1	0,1	40,2	24,2	Segmento 2, Micropilote 40	3	159	8,1	40,2	24,2
	Segmento 3, Micropilote 40	4	157	42,3	0,0	10,3	0,1	39,8	25,0	Segmento 3, Micropilote 40	4	157	10,3	39,8	25,0
	Segmento 4, Micropilote 40	13	163	42,3	0,1	34,7	0,1	41,2	38,0	Segmento 4, Micropilote 40	13	163	34,7	41,2	38,0
	Segmento 5, Micropilote 40	13	160	42,3	0,1	34,7	0,1	40,6	37,7	Segmento 5, Micropilote 40	13	160	34,7	40,6	37,7
	Segmento 6, Micropilote 40	21	159	42,3	0,1	57,0	0,1	40,3	48,6	Segmento 6, Micropilote 40	21	159	57,0	40,3	48,6
	Segmento 7, Micropilote 40	26	158	42,3	0,1	70,5	0,1	40,0	55,3	Segmento 7, Micropilote 40	26	158	70,5	40,0	55,3
	Segmento 8, Micropilote 40	22	156	42,3	0,1	60,5	0,1	39,6	50,0	Segmento 8, Micropilote 40	22	156	60,5	39,6	50,0
	Segmento 9, Micropilote 40	19	157	42,3	0,1	51,0	0,1	39,8	45,4	Segmento 9, Micropilote 40	19	157	51,0	39,8	45,4
	Segmento 10, Micropilote 40	21	157	42,3	0,1	55,9	0,1	39,8	47,8	Segmento 10, Micropilote 40	21	157	55,9	39,8	47,8
	Segmento 11, Micropilote 40	18	159	42,3	0,1	47,7	0,1	40,2	44,0	Segmento 11, Micropilote 40	18	159	47,7	40,2	44,0
	Segmento 12, Micropilote 40	26	262	42,3	0,1	70,0	0,1	66,4	68,2	Segmento 12, Micropilote 40	26	262	70,0	66,4	68,2

Appendix D | Typical Load Test Setup


Appendix F | Comparison with FHWA estimations

			Predictive ASD	Predictive | LRFD			FHWA		
Depth (m)	P_{ult} (kN)	FS	P_{allow} (kN)	Pall (kN), $\phi = 0,5$	Pall (kN), $\phi = 0,55$	Pall (kN), $\phi = 0,65$	P_{allow} (kN), min	P_{allow} (kN), aver	P_{allow} (kN), max
1	13,8	2	6,9	6,9	7,6	9,0	0,0	0,0	0,0
2	39,6	2	19,8	19,8	21,8	25,7	11,0	20,4	22,0
3	65,4	2	32,7	32,7	36,0	42,5	22,0	40,8	44,0
4	108,7	2	54,3	54,3	59,8	70,6	34,1	63,3	68,2
5	151,9	2	76,0	76,0	83,6	98,8	46,2	85,8	92,4
6	188,6	2	94,3	94,3	103,7	122,6	65,2	116,9	133,8
7	225,2	2	112,6	112,6	123,9	146,4	84,2	148,0	175,3
8	283,2	2	141,6	141,6	155,8	184,1	104,9	181,9	220,5
9	341,2	2	170,6	170,6	187,7	221,8	125,7	215,8	265,8
10	402,9	2	201,4	201,4	221,6	261,9	146,4	249,8	311,0
11	464,5	2	232,2	232,2	255,5	301,9	167,1	283,7	356,3
12	522,5	2	261,2	261,2	287,4	339,6	187,9	317,6	401,5